

NO-A177 368

NUCLEAR WEAPONS EFFECTS STUDIES FOR THE SESS
(TRADEMARK) SWITCH VOLUME 2 (U) AT AND T TECHNOLOGIES
INC GREENSBORO NC W A BEAUCHAMP ET AL SEP 86

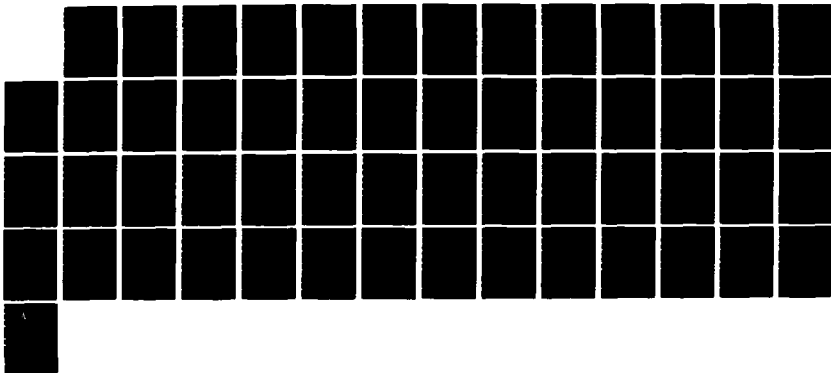
1/1

UNCLASSIFIED

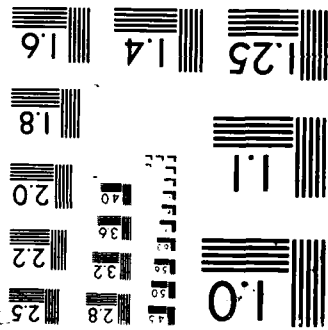
NCS-TIB-86-3-VOL-2 DCA100-85-C-0094

F/G 9/1

NL



MICROCOPY RESOLUTION TEST CHART
1010A



2

NCS TIB 86-3



NATIONAL COMMUNICATIONS SYSTEM

AD-A177 368

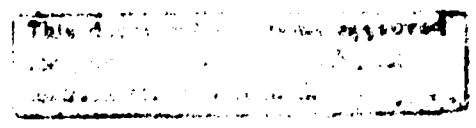
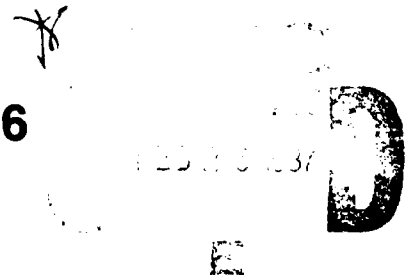
**TECHNICAL INFORMATION BULLETIN
86-3**

**NUCLEAR WEAPONS EFFECTS STUDIES
FOR THE 5ESS™ SWITCH**

**VOLUME II: EM SHIELDING
CHARACTERISTICS OF STRUCTURES**

FILE COPY

SEPTEMBER 1986



87 2 24 028

REPORT DOCUMENTATION PAGE

Form Approved
OMB No 0704-0188
Exp Date Jun 30, 1986

1a REPORT SECURITY CLASSIFICATION Unclassified		1b RESTRICTIVE MARKINGS	
2a SECURITY CLASSIFICATION AUTHORITY Not Applicable		3 DISTRIBUTION/AVAILABILITY OF REPORT A - Unlimited	
2b DECLASSIFICATION/DOWNGRADING SCHEDULE Not Applicable		4 PERFORMING ORGANIZATION REPORT NUMBER(S) None	
6a NAME OF PERFORMING ORGANIZATION AT&T Technologies, Inc.		6b OFFICE SYMBOL (if applicable) NCS-TS	
6c ADDRESS (City, State, and ZIP Code) Guilford Center P. O. Box 20046 Greensboro, NC 27420		7a NAME OF MONITORING ORGANIZATION National Communications System Office of Technology and Standards	
7b ADDRESS (City, State, and ZIP Code) Attn: NCS-TS Washington, DC 20305-2010		5 MONITORING ORGANIZATION REPORT NUMBER(S) NCS TIB 86-3	
8a NAME OF FUNDING/SPONSORING ORGANIZATION National Communications System		8b OFFICE SYMBOL (if applicable) NCS-TS	
8c ADDRESS (City, State, and ZIP Code) See Item 7b.		9 PROCUREMENT INSTRUMENT IDENTIFICATION NUMBER DCA100-85-C-0094	
10 SOURCE OF FUNDING NUMBERS			
PROGRAM ELEMENT NO. 33127K	PROJECT NO.	TASK NO.	WORK UNIT ACCESSION NO.
11. TITLE (Include Security Classification) Nuclear Weapons Effects Studies for the SESS™ Switch Volume II: EM Shielding Characteristics of Structures			
12 PERSONAL AUTHOR(S) N. A. Beauchamp, L. Farber, S. S. Federico			
13a TYPE OF REPORT Final Report	13b TIME COVERED FROM 85-01-07 TO 86-09-30	14 DATE OF REPORT (Year, Month, Day) 86-09	15 PAGE COUNT 53
16 SUPPLEMENTARY NOTATION Prepared by AT&T Bell Laboratories on behalf of AT&T Technologies, Inc.			
17 COSATI CODES			18 SUBJECT TERMS (Continue on reverse if necessary and identify by block number) EMP SESS™ Switch EM Shielding
FIELD	GROUP	SUB-GROUP	
19 ABSTRACT (Continue on reverse if necessary and identify by block number) <p>As part of its Electromagnetic Pulse (EMP) Mitigation Program, the National Communications System (NCS) funded AT&T to study the ability of the AT&T SESS™ Switch to withstand the potentially disabling effects of EMP from high-altitude nuclear bursts and fallout radiation from distant near-surface bursts.</p> <p>This volume documents the study to characterize the electromagnetic (EM) shielding effectiveness of the trailer used to shelter the test switch during simulated-EMP testing and of central-office buildings in which SESS Switches might be housed in the Public Switched Network. The results were used to estimate the attenuated fields incident upon n installed switch and its associated intra-office cabling. Because the building types examined can provide a wide range of EM shielding values, no single set of attenuation curves will suffice to characterize central-office structures.</p>			
20 DISTRIBUTION/AVAILABILITY OF ABSTRACT <input type="checkbox"/> UNCLASSIFIED/UNLIMITED <input checked="" type="checkbox"/> SAME AS RPT. <input type="checkbox"/> DTIC USERS		21 ABSTRACT SECURITY CLASSIFICATION Unclassified	
22a NAME OF RESPONSIBLE INDIVIDUAL Andre H. Rausch		22b TELEPHONE (Include Area Code) (202) 692-2124	22c OFFICE SYMBOL NCS-TS

NCS TECHNICAL INFORMATION BULLETIN 86-3

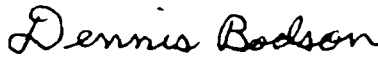
NUCLEAR WEAPONS EFFECTS STUDIES FOR THE SESSTM SWITCH (U)

SEPTEMBER 1986

PROJECT OFFICER


ANDRE RAUSCH
Electronics Engineer
Office of Technology
and Standards

APPROVED FOR PUBLICATION:


DENNIS BODSON
Assistant Manager
Office of Technology
and Standards

FOREWORD

The National Communications System (NCS) is an organization of the Federal Government whose membership is comprised of 22 Government entities. Its mission is to assist the President, National Security Council, Office of Science and Technology Policy, and Office of Management and Budget in:

- o The exercise of their wartime and non-wartime emergency functions and their planning and oversight responsibilities.
- o The coordination of the planning for and provision of National Security/Emergency Preparedness communications for the Federal Government under all circumstances including crisis or emergency.

In support of this mission the NCS has initiated and manages the Electromagnetic Pulse (EMP) Mitigation Program. The major objective of this program is to significantly reduce the vulnerability of the U.S. telecommunication infrastructure to disabling damage due to nuclear weapon effects in direct support of the survivability and endurability objectives addressed by Executive Order 12472 and National Security Decision Directive 97. Nuclear weapon effects include EMP, magnetohydrodynamic EMP (MHD-EMP), and fallout radiation from atmospheric detonations. The purpose of this Technical Information Bulletin is to provide the reader with information relating to specific areas of EMP which are being investigated in support of the NCS EMP Mitigation Program.

Comments on this TIB are welcome and should be addressed to:

Office of the Manager
National Communications System
ATTN: NCS-TS
Washington, DC 20305-2010
(202) 692-2124

FIGURES

Figure 2-1.	Vertical electric-field measurements on trailer — 0.01 to 1.01 MHz.....	7
Figure 2-2.	Vertical electric-field measurements on trailer — 1 to 31 MHz.....	8
Figure 2-3.	Vertical electric-field measurements on trailer — 30 to 130 MHz.....	9
Figure 2-4.	Horizontal electric-field measurements on trailer — 30 to 130 MHz.....	10
Figure 2-5.	Typical magnetic-field measurements on trailer.....	11
Figure 3-1.	Electric-field attenuation — single-family residence with wood and brick siding (Building Type 1).....	21
Figure 3-2.	Electric-field attenuation — single-family residence with aluminum siding (Building Type 2).....	22
Figure 3-3.	Electric-field attenuation — single-story concrete-block (Building Type 3).....	23
Figure 3-4.	Electric-field attenuation — single-story concrete-block (Building Type 4).....	24
Figure 3-5.	Electric-field attenuation — four-story office building (Building Type 5).....	26
Figure 3-6.	Electric-field attenuation — four-story office building (Building Type 6).....	27
Figure 3-7.	Electric-field attenuation — twenty-story office building (Building Type 7).....	28

TABLES

Table 2-1.	TEST EQUIPMENT USED TO DETERMINE TRAILER SHIELDING VALUES.....	5
Table 3-1.	ELECTRIC-FIELD ATTENUATION OF TWO 2ESS PRECAST CONCRETE BUILDING SITES.....	17
Table 3-2.	ELECTRIC-FIELD ATTENUATION OF THREE 5ESS™ BUILDING SITES.....	18
Table 3-3.	ASYMPTOTIC SHIELDING ATTENUATION VALUES USED IN FITTING ANALYSIS (AT LOW FREQUENCIES).....	32
Table 3-4.	PEAK INTERNAL ELECTRIC FIELDS FOR VARIOUS BUILDING TYPES (NO FLOOR/GROUND REFLECTIONS).....	33
Table 3-5.	PEAK INTERNAL ELECTRIC FIELDS FOR VARIOUS BUILDING TYPES AT A HEIGHT OF 2 METERS ABOVE REFLECTING FLOOR/GROUND WITH $\sigma = 0.01$ MHO/METER.....	36
Table 3-6.	PEAK CURRENTS ON CABLES 2 METERS ABOVE FLOOR FOR 1-KV/METER INCIDENT FIELDS ($\sigma = 0.01$ MHO/METER).....	37
Table 3-7.	PEAK CURRENTS PREDICTED FOR CABLES 2 METERS ABOVE FLOOR/GROUND IN ABSENCE OF BUILDINGS (1-KV/METER INCIDENT FIELD).....	38
Table 4-1.	EFFECTS OF BUILDING SHIELDING FACTORS ON PEAK CABLE CURRENTS.....	41

1. INTRODUCTION

1.1 Background

The provision of telecommunication services during national emergency situations is critical if this country is to continue functioning as a viable entity during such periods. The National Communications System (NCS) plays a key role in ensuring that such services will be available to Government agencies. In particular, the NCS is currently implementing programs consistent with National Security Decision Directive 97 of 1983, in which the NCS was directed to develop an architecture for a survivable/enduring communications system. These programs reflect a reliance on the Public Switched Network (PSN) to meet such communications needs, as per the instructions of Executive Order #12472 of April 3, 1984.

In accord with the above, the NCS has initiated a Nationwide Emergency Telecommunications System (NETS) study to ascertain if surviving PSN resources might be utilized to meet essential Government communications needs during a protracted national emergency. Task 3 of that effort provided for a field demonstration of a skeletal NETS using pre-prototype hardware and software; a separate contractual effort (under Contract Number DCA100-85-C-0059) initiated the work needed to ensure survival of NETS hardware to the effects of nuclear bursts (see Reference 1). The NETS program does not, however, provide a means for determining the susceptibility of the various elements of the PSN to a nuclear laydown. In light of this, the NCS has funded AT&T under Contract Number DCA100-85-C-0094 to determine the ability of the AT&T *5ESS*TM Switch to withstand the potentially disabling effects of the electromagnetic pulse (EMP) from high-altitude bursts and the fallout radiation from distant near-surface bursts. The effort is part of the NCS EMP Mitigation Program, formulated to characterize the behavior of the PSN upon exposure to nuclear environments.

This study of the *5ESS* Switch is relevant and important because existing projections indicate that it will provide a growing fraction of PSN telephone exchanges. Thus, a hardness assessment of the *5ESS* Switch is one of the several studies needed to determine what PSN resources will actually be available for incorporation into a viable NETS during and after a nuclear emergency. Another important reason for undertaking a hardness assessment of the *5ESS* Switch is the potential role of this switch in the Defense Switched Network (DSN) of the Department of Defense (DoD).

1.2 Scope of Study Effort

The overall contractual effort addressed two somewhat different sets of issues: first, the determination of the behavior of a "standard" (unhardened) *5ESS* Switch, typical of a rural or suburban installation, upon exposure to a high-altitude EMP (HEMP) environment; and, second, a preliminary evaluation of the fallout-radiation susceptibility of a *5ESS* Switch and the generation of a detailed Radiation Hardness Assessment Plan. A four-task effort was structured to address these

issues. The fourth of these tasks encompassed the fallout-radiation studies, the results of which are presented in Volume IV of the four-volume Final Technical Report that completes the documentation requirements of the aforementioned contract.

Volume I of the Final Technical Report presents an executive summary of the entire contractual effort; Volume III contains the results obtained from addressing the second and third tasks, which were concerned with analyses and tests to determine the response of a small *5ESS* Switch upon exposure to a HEMP environment. This document, which constitutes Volume II of the Final Technical Report, discusses the activities on the first task of the contractual effort: a study of the shielding afforded to HEMP-like fields by structures typical of those that might be used to house operational rural or suburban *5ESS* Switches and a determination of the electromagnetic (EM) attenuation provided by the trailer that was used to house the test switch during exposure to simulated-EMP fields. This document, therefore, provides critical input to the process that attempts to relate the observed behavior of the test *5ESS* Switch under the EMP simulators to that which might be expected from a switch subjected to HEMP in an operational site: it compares the transients induced by HEMP-like fields within the test trailer with those expected within typical office structures that could be used to house rural or suburban *5ESS* Switches.

Section 2, following, discusses the attenuation afforded by the aforementioned trailer to HEMP-like fields and presents the results of calculations characterizing currents induced by these fields on conductors inside the trailer. These currents are compared with those that would be expected in the absence of the trailer. Section 3 then proceeds to present similar information for several types of buildings that might be used to house an operational *5ESS* Switch. Section 4 puts these results into perspective. Appendices at the end of the volume give the reader insight into some of the tools used in the analysis.

2. TRAILER SHIELDING ANALYSIS

2.1 Nature of Problem

The small *5ESS* Switch assembled as part of this program and exposed under the ALECS and Horizontally Polarized Dipole (HPD) EMP simulators at the Air Force Weapons Laboratory (AFWL) was housed in a trailer covered with fiberglass-clad plywood. This trailer provided environmental protection and a structurally sound envelope for the test unit. The switch underwent several weeks of testing at the AFWL facilities. For each pulse, information was recorded as to the behavior of the switch and the transients induced on a variety of cables within and leading to the switch. The details of those experiments are discussed in Volume III of this Final Technical Report. Although of more than passing interest, it should be noted that the behavior of the switch observed under a particular field level at ALECS or HPD is not the final issue: we are concerned with the behavior of an operational *5ESS* Switch housed in a PSN building when the building is subjected to a threat-level EMP environment. Obviously, a necessary step in determining this latter behavior is the prediction of transients on cables in an operational site. We assert that the following expression allows one to predict the nature of such a threat-level transient $g_t(t)$:

$$g_t(t) = \frac{1}{2\pi} \int_{-\infty}^{\infty} \bar{g}_t(\omega) e^{-i\omega t} d\omega, \quad (2.1)$$

where $\bar{g}_t(\omega)$ is the Fourier transform (FT) of $g_t(t)$ given by

$$\bar{g}_t(\omega) = \bar{f}_t(\omega) [\bar{g}_{exp}(\omega) / \bar{f}_{exp}(\omega)], \quad (2.2)$$

with

$$\bar{f}_t(\omega) = \text{FT of threat field seen by the cable,}$$

$$\bar{f}_{exp}(\omega) = \text{FT of driving field in the test,}$$

and

$$\bar{g}_{exp}(\omega) = \text{FT of transient seen when cable is subjected to } \bar{f}_{exp}(\omega).$$

In many cases, the cables of interest are those that were located at least partially inside the trailer and are nominally within a PSN building. In these cases, the driving fields $\bar{f}_t(\omega)$ and $\bar{f}_{exp}(\omega)$ are *not* the fields incident upon the trailer and building but, rather, those that are seen interior to these structures. Thus, if we define $a_{tr}(\omega)$ and $a_{bldg}(\omega)$ as the frequency-dependent transfer functions for the trailer and building, respectively, we have

$$\bar{g}_t(\omega) = [\bar{f}_{t,e}(\omega) \times a_{bldg}(\omega)] \times \left\{ \bar{g}_{exp}(\omega) / [\bar{f}_{exp,e}(\omega) \times a_{tr}(\omega)] \right\}, \quad (2.3)$$

where $\tilde{f}_{t,e}(\omega)$ is the FT of the threat-level field incident upon the building that houses the operational switch and $\tilde{f}_{exp,e}(\omega)$ is the FT of the ALECS or HPD field incident upon the trailer. In the above expression $\tilde{f}_{exp,e}(\omega)$ is available for each test shot, $\tilde{g}_{exp,e}(\omega)$ is obtained from the experimental records, and $\tilde{f}_{t,e}(\omega)$ is the FT of the (assumed known) threat-level field. Thus, evaluation of the above equation further requires only a knowledge of $a_{tr}(\omega)$ and $a_{bldg}(\omega)$. This section discusses our attempts to evaluate $a_{tr}(\omega)$ and its use in the analysis of the simulation test data. Section 3, following, performs a similar function for $a_{bldg}(\omega)$.

Although the driving fields of concern to an EMP analysis include both the magnetic and electric fields, we will be restricting our attention primarily to the electric fields. Previous work (such as that in Reference 1) has shown that the major currents of concern to typical telephone installations are usually those driven by the electric fields.

2.2 Experimental Data

The trailer used to house the small *SESS* Switch during the tests at AFWL was 12.2 meters (40 feet) long, 2.4 meters (8 feet) wide, and 2.9 meters (9.5 feet) high. The walls and top of the trailer were made of fiberglass reinforced plywood to reduce the expected EM attenuation values for the trailer. The plywood was mounted on the existing open steel-beam support structure of the trailer. Further details on the trailer are found in Volume III of this report.

Before assembling the switch in the trailer at the AT&T Bell Laboratories Indian Hill location, we subjected the trailer to a series of tests to determine the shielding effectiveness of this structure against electric and magnetic fields. Although the switch was not in place, the trailer contained essentially all the ancillary wiring for lights, etc. For the tests, the trailer was located some 40 meters from the Indian Hill open-field test site. Shielding effectiveness tests were performed over the frequency range between 10 kHz and 100 MHz for electric fields and between 10 kHz and 30 MHz for magnetic fields. Table 2-1 lists the test equipment used.

The basic approach used in these tests was to measure the received power using a receive antenna and a transmit antenna in two experimental configurations that differed only in the presence or absence of a trailer wall between the two antennae. The difference in received power was then ascribed to attenuation by the trailer. The tests were performed using an essentially continuous-wave (CW) source at each of a large number of frequencies to provide a frequency-dependent transfer function for the trailer.

The two antennae were first set up outside and away from the trailer at a fixed horizontal separation distance and height above the ground. The separation distance was 1 meter for all measurements except the electric-field measurements taken between 30 and 100 MHz, for which the separation was set equal to 10 meters. The antenna height above ground was 2.3 meters, with

Table 2-1. TEST EQUIPMENT USED TO DETERMINE TRAILER SHIELDING VALUES

Equipment	Model Number
HP Spectrum Analyzer	Model 8568A
HP Synthesized Signal Generator	Model 8662A
HP Desktop Computer	Model 9826
HP Plotter	Model 9872C
Singer Loop Antenna	Model LG-105A
Empire Loop Antenna	Model LG-205
Singer Loop Antenna	Model LP-105SC
Empire Loop Antenna	Model LP-205
Singer Active Whip Antenna	Model 95010-1
Amplifier Research E-Field Generator	Model AT-3000
EMCo Biconical Antenna	Model 3104
EMCo Biconical Antenna	Model 3109

antenna height being defined as the distance from the ground to the bottom of the rod of the active rod antenna and to the center of all other antennae. This height setting was selected so that, in the subsequent measurements made with the trailer in place, the main antenna pattern would be centered about halfway up the trailer wall. Using a convenient output signal level on the signal generator driving the transmit antenna, we measured the received power, in dBm, as the frequency of the transmitted signal was swept over a suitable frequency range. The frequency range was swept in 1000 steps with a dwell time of 10 milliseconds per step.

The receive antenna was then placed inside the trailer and the transmit antenna was moved so as to maintain the same horizontal separation as used for the free-field (no-trailer) measurements. Using the same signal to drive the transmit antenna and the same cable lengths as for the no-trailer case, we again measured the received power, in dBm, as the frequency was swept.

The trailer was outfitted with double doors at the rear to ease the moving of equipment in and out. In addition, a personnel-access door was installed at about the midpoint of one side (in the right-hand 12.2-meter-long wall of the trailer, as one faces forward). The receive and transmit antennae were located so as to measure the attenuation provided by the longitudinal wall opposite from the side with the access door.

Measurements with the receive antenna inside the trailer were taken at three locations. For all three, the receive antenna was 1 meter above the trailer floor (which was 1.3 meters above the ground level) and 0.5 meter from the wall facing the transmit antenna. The three locations selected for the measurements were those for which the antennae were centered at distances of 2.7 meters,

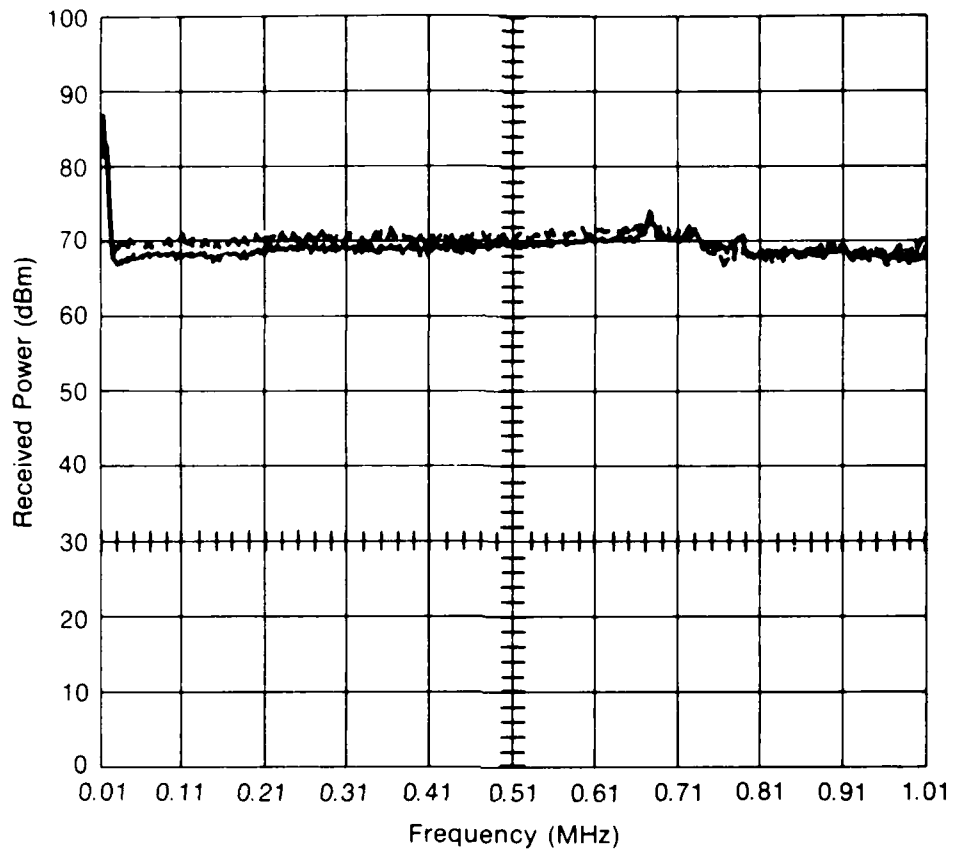
5.9 meters, and 10.4 meters from the rear doors of the trailer. These positions were selected to give insight into the variation of the attenuation along the length of the trailer.

Selected results from the measurements are presented in Figures 2-1 through 2-5. In these figures, the dashed or broken lines represent data taken without the trailer wall between the two antennae. The solid lines show the results of measurements for the case where the receive antenna was inside the trailer at a point 5.9 meters from the rear of the trailer, i.e., for a point about midway between the front and rear. The results for the two other locations in the trailer were very similar to those shown for the 5.9-meter location. Thus, the conclusions drawn below are deemed valid for all internal points.

From the data shown in Figures 2-1 through 2-5, we can draw the following conclusions.

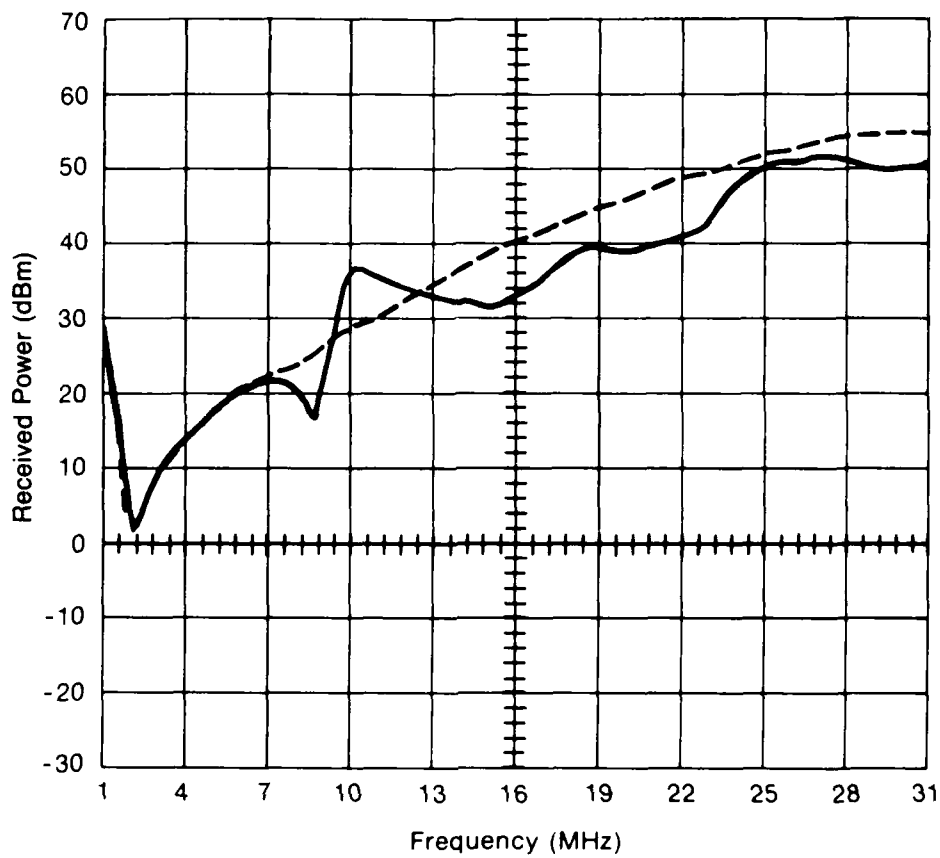
- For the low-frequency region below about 7 MHz, the trailer afforded little discernible attenuation to the incident vertically polarized electric fields (see Figures 2-1 and 2-2).
- For the electric field at frequencies between about 7 MHz and 85 MHz, there was, however, a noticeable effect of the trailer on the received power. Maximum departures from the no-trailer case are as large as about 8 dB, with both enhancements and degradations being present.
- At frequencies above about 85 MHz, again, the trailer seemed to have essentially no effect on the received electric-field intensity.
- Figure 2-4 shows some of the data obtained when the electric-field polarization was changed from vertical to horizontal. Comparison of the data with those of Figure 2-3 indicates that the attenuation provided by the trailer to electric fields was only weakly dependent upon the polarization direction.
- The data of Figure 2-5 are quite characteristic of the entire set of magnetic-field measurements. The trailer is seen to have had very little effect on the received power of the magnetic fields.

Thus, we conclude that the impact of the trailer on incident EM fields was small and was confined primarily to effects on the electric field in the frequency range between about 7 and 85 MHz. However, it is noted that, even in this range of greatest departure from the free-field (no-trailer) case, the behavior was not that of simple absorption. Rather, the behavior was more like that of a system for which the receive antenna is picking up the direct radiated wave plus moderately strong reflected waves—the received power for such a case would show oscillatory frequency-domain behavior with alternate enhancements and degradations in the received power relative to that in the direct radiation alone. The behavior of the data between 7 and 85 MHz can be moderately well described by such a pattern.



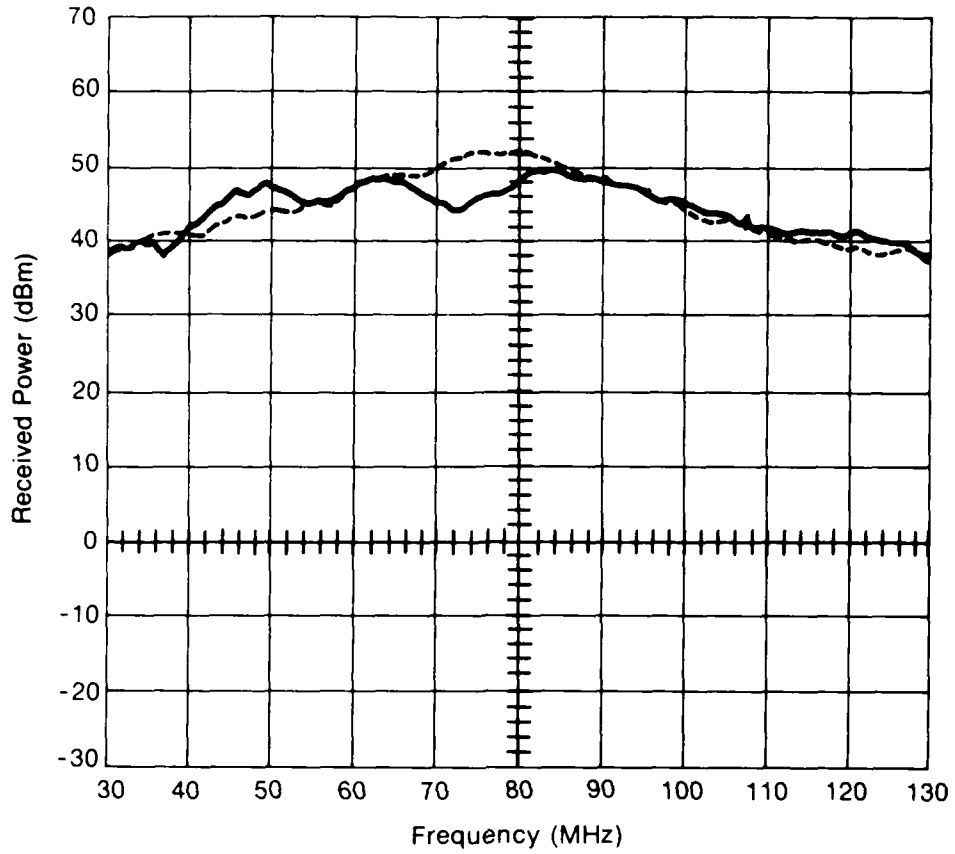
Broken Line: Outside Measurement
 Solid Line: Inside Measurement

Figure 2-1. Vertical electric-field measurements on trailer — 0.01 to 1.01 MHz.



Broken Line: Outside Measurement
 Solid Line: Inside Measurement

Figure 2-2. Vertical electric-field measurements on trailer – 1 to 31 MHz.



Broken Line: Outside Measurement
 Solid Line: Inside Measurement

Figure 2-3. Vertical electric-field measurements on trailer — 30 to 130 MHz.

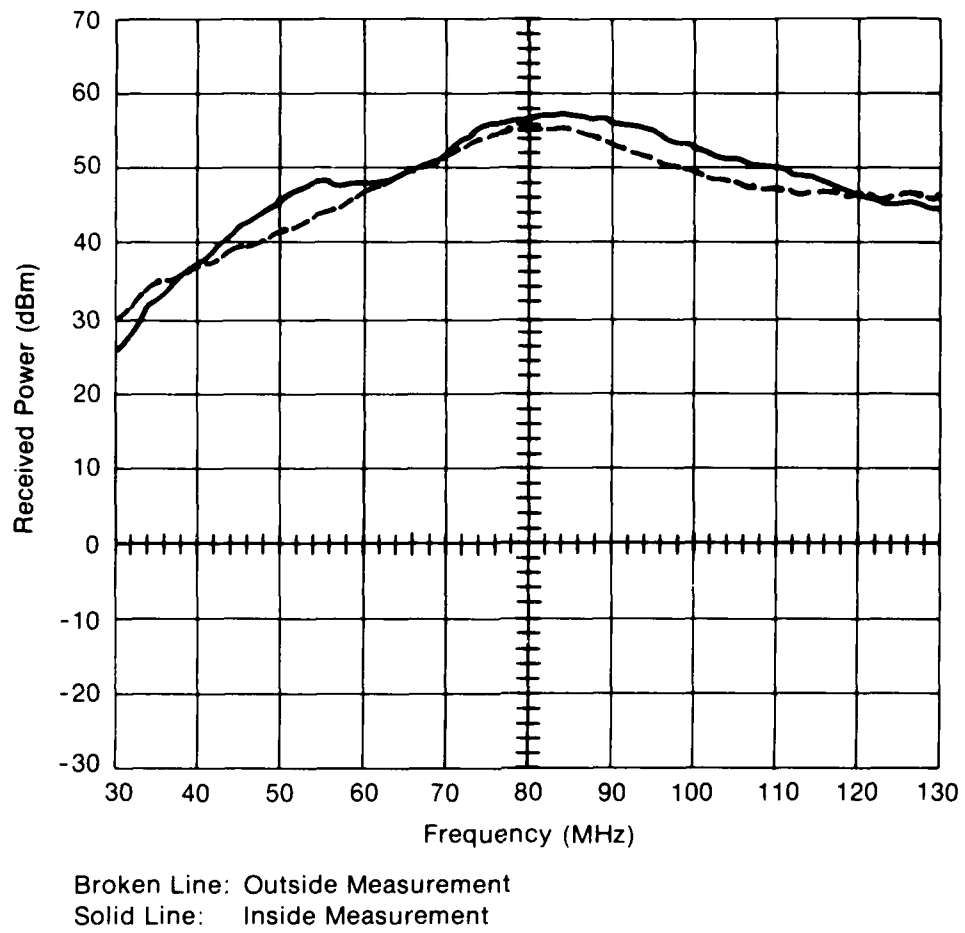
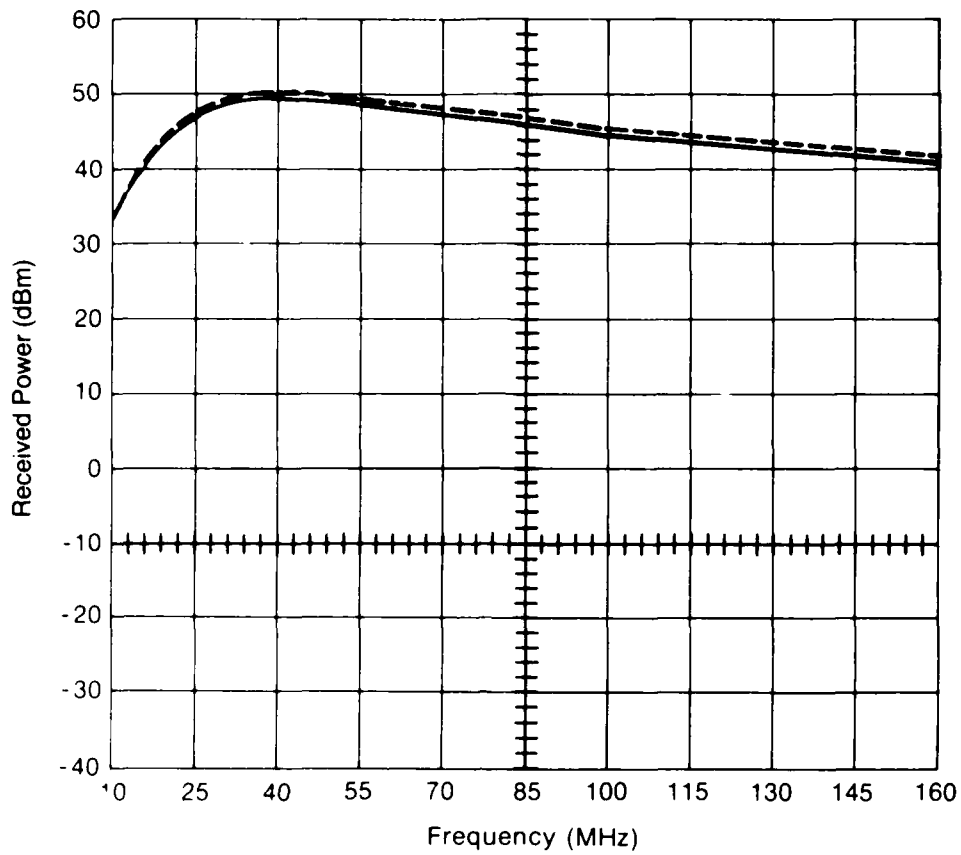


Figure 2-4. Horizontal electric-field measurements on trailer — 30 to 130 MHz.



Broken Line: Outside Measurement
 Solid Line: Inside Measurement

Figure 2-5. Typical magnetic-field measurements on trailer.

To verify that no significant absorptive process was present, we also made measurements on the fiberglass-clad plywood that made up the sides of the trailer. The results of those measurements showed that there was no discernible effect of this material on either electric or magnetic fields in the frequency range of the test equipment.

The measured data are used in the paragraphs below to derive quantitative estimates of the attenuation afforded by the trailer to EMP-like pulses.

2.3 Effects on EMP-Like Fields

The data discussed above show that the only significant effects of the trailer on an incident EM signal will be confined to the electric-field components at frequencies between about 7 and 85 MHz. Since most of the energy of the simulated-EMP fields at the ALECS and HPD facilities lies at energies below 7 MHz, the energy content of the field internal to the trailer at an AFWL facility will be very close to that of the incident field. However, the spectral content of the interior field will be slightly different from that of the incident field. Therefore, the currents induced on cables within the trailer will be somewhat different. We wish to quantify what these differences might be. To accomplish this, we constructed a transfer function $a_{tr}(\omega)$ consistent with the measured data for the electric-field component of an EM wave and used this function to calculate the effects of the trailer on the peak currents expected on shorted cables of 1, 10, and 50 meters located inside the trailer, relative to the peak currents one would expect if the cables were exposed directly to the fields incident upon the trailer. On cables of various lengths, peak value-differences in the short-circuit current indicate a structure's significant shielding effects.

The first step in this procedure consisted of an effort to derive a complex frequency-dependent transfer function $a_{tr}(\omega)$ that matched the experimental data. To this end, we expressed the transfer function as a sum of analytic functions to fit the measured data with

$$a_{tr}(\omega) = \frac{1}{2} \sum_n A_n \left\{ \frac{1}{(-i\omega - \alpha_n)^2} + \frac{1}{(-i\omega - \alpha_n^*)^2} \right\}, \quad (2.4)$$

where each α_n is a complex pole in the ω -plane and A_n is a real coefficient. With this definition of $a_{tr}(\omega)$, we selected the α_n and A_n values to give the best fit to the measured data, where it should be noted that the difference between the two curves plotted in Figures 2-1 through 2-3 is merely the quantity

$$-20 \log |a_{tr}(\omega)|.$$

We chose the above form for $a_{tr}(\omega)$ to ensure the use of a complex analytic transfer function consistent with physical processes. (See Appendix A for a short discussion of the fit used in this approach.)

The resulting fit for $a_{tr}(\omega)$ was used to calculate the interior fields and peak interior cable currents for two incident wave forms: a double-exponential wave given by

$$f(t) = e^{-\alpha t} - e^{-\beta t}$$

with $\alpha = 4 \times 10^6/\text{second}$ and $\beta = 4.76 \times 10^8/\text{second}$, and a zero-rise-time, single-exponential form given by

$$f(t) = e^{-\alpha t}$$

with $\alpha = 4 \times 10^6/\text{second}$. We could have used sample ALECS and HPD waveforms, but the convolution of the two exponential waveforms above with the analytic fit chosen for the transfer function has one significant advantage: the time- and frequency-domain solutions for the interior fields assume rather simple closed forms. In addition, it should be noted that the simulated-EMP fields are sufficiently like the double-exponential waveform that the conclusions drawn below are deemed valid for these more complex waveforms.

We used the closed-form solutions referred to above to calculate cable currents using the formalism presented in Appendix A.3 of Reference 1 and Appendix B of this report.

The results of our investigations are summarized in the following points.

- The energy content of the internal electric field was calculated to be within 0.1 dB of that in the incident field.
- The peak value of the internal electric field was also calculated to be within 0.1 dB of that for the external, incident field.
- Peak currents on the shorted 1-meter cable were calculated to be some 1.6 dB smaller inside the trailer relative to those predicted for cables exposed directly to the incident field. This corresponds to a 17-percent decrease in peak current value and was found to constitute the largest effect of the trailer shell on any internal transient.
- The corresponding decrease in the peak currents calculated for the 10-meter cable was about 1.0 dB (corresponding to a 10-percent decrease in amplitude).
- The 50-meter cable showed a negligible decrease in predicted peak current.
- The results cited above were the same for both incident waveforms used.
- The internal field calculated from the analytic fit to $a_{tr}(\omega)$ had the general characteristics of a slightly attenuated direct wave plus a reflected wave (consistent with our earlier comments on the frequency-domain behavior of the experimental data).

The above observations were all made for the case in which the wave interior to the trailer undergoes no reflections off the floor, which consisted of wood over steel support members. At ALECS, the effects of the conducting floor are minimal in perturbing the incident vertically polarized wave that assumes its double-exponential-like form specifically because of the presence of a conducting ground plane. This makes the no-reflection case quite appropriate for tests at ALECS. However, the presence of a partially reflecting floor or ground plane inside the trailer at the HPD can change markedly the field seen by a cable within the test trailer from the attenuated double-exponential-like wave radiated by the biconic antenna. Thus, we also made calculations for the case where the horizontal component of the internal electric field is subject to reflections from the trailer floor so that the interior cables are subjected not only to the attenuated incident field but also its reflection. Our calculations showed that, for such cases, the peak electric field seen inside the trailer is decreased by some 20 to 30 percent (depending on the reflectivity of the ground plane interior to the trailer) relative to that expected for an absolutely inert trailer shell over the same ground plane. However, the effects of the trailer shell on internal cable currents are no more pronounced than those cited above in the absence of ground or floor reflections. In fact, the peak cable currents predicted for the 10-meter cable exhibit an even smaller decrease due to the presence of the trailer shell when reflections from the floor are present than when ground-plane reflections are absent.

Thus, we conclude that the trailer has minimal effect on peak fields and cable currents, and we feel quite justified in neglecting the shielding effects of the trailer in interpreting the experimental data obtained at AFWL. This means we can, to a high degree of accuracy, simplify Equation (2.3) of Section 2.1 by replacing $a_{tr}(\omega)$ by unity.

3. BUILDING SHIELDING ANALYSIS

3.1 Nature of Problem

As shown in the previous section, the trailer used to house the *5ESS* Switch tested at AFWL exhibited negligible attenuation of incident EMP-like fields. Thus, measurements of transients upon exposure to known ALECS and HPD fields can be used to predict transients induced under threat-level conditions for *5ESS* Switches in operational sites from a somewhat simplified form of Equation 2.3,

$$\tilde{g}_i(\omega) = \left[\tilde{f}_{i,e}(\omega) \times a_{\text{bldg}}(\omega) \right] \times \left[\tilde{g}_{\text{exp}}(\omega) / \tilde{f}_{\text{exp,e}}(\omega) \right], \quad (3.1)$$

if we can determine the frequency-dependent building transfer function $a_{\text{bldg}}(\omega)$. (See Section 2 for a definition of the other terms in the above equation.)

The buildings of interest for this study are those that house current and future *5ESS* Switches in rural and small suburban PSN installations. If a standard building design existed for such installations, measurements taken on a single such building would suffice to meet our needs. Unfortunately, no such standard exists; for example, the desire to have telephone buildings blend in with other buildings in the vicinity has given rise to a wide variety of architectural styles for structures housing PSN switches. In spite of the lack of a standard building type for housing *5ESS* Switches of interest, however, it was determined that most rural and small suburban offices are (and will be) single-story structures. Thus, we embarked upon an extensive literature search to determine what data base exists for characterizing the EM shielding effectiveness of such buildings. (See the bibliography at the end of this paper for a partial list of the literature consulted.) This section reports on the findings of that literature search and on the use of the available data-base to calculate building shielding effectiveness values for incident EMP-like fields.

We initially planned to report only on the findings for the single-story building types of primary concern in this study. However, our work uncovered information on multi-story building types that could be used to house *5ESS* or other PSN equipment in urban and large suburban installations. Since the overall activities of the NCS also reflect concern about the behavior of PSN equipment at such sites, we have elected to incorporate information on these larger building types in this document. We hope that the data will be useful in future studies.

3.2 Results of Literature Search

3.2.1 Survey of PSN Installations. Our search for information on the shielding effectiveness of buildings that could be used to house a rural or small suburban *5ESS* Switch was first directed at a determination of the building types that already contain such switching equipment. We found that the current locations of such switches can indeed be determined, as can be the locations of those

scheduled for near-future installation. However, in the post-divestiture environment, the projected long-term deployment of 5ESS Switches by the regional operating companies is not readily available to AT&T; but we *did* find that many of the planned switches would probably be installed in existing buildings (either as additions to or replacements of existing switching facilities). Thus, our efforts to characterize the types of buildings that can be used to house the 5ESS Switch centered on a survey of those units that had been placed in service by December 1985 (15 in the toll PSN and 91 in the local networks administered by the regional operating companies) *plus* selected rural and suburban offices that currently contain other switching equipment (such as the AT&T 2ESSTM Switch) and which could house 5ESS installations in the future.

The resulting survey showed that a rural or suburban switching office is typically a single-story, concrete-block building, perhaps with some metal reinforcement. For example, the Warrenville, Illinois, central office building is a single-story structure. The monolithic roof and columns of this building are of poured reinforced concrete; and the non-load-bearing walls are made of brick and concrete block. The floor is a reinforced concrete slab, poured on grade. The building does contain rebar, but they are not intentionally tied together, nor are they connected to ground.

Having identified this general characterization of the building type that can be expected to house a rural or small suburban 5ESS Switch, we then tried to determine what measurements had been taken to describe the EM shielding provided by such buildings in the PSN. Only limited measurements seem to have been taken; but we did find that a study had been made of the EM shielding levels for two "standard" Illinois Bell 2ESS buildings located in the suburban Chicago area. These buildings, located in Romeoville and Frankfort, Illinois, are single-story structures of approximately 5000 square feet, with poured-in-place concrete foundations, precast concrete sidewall panels, prestressed concrete roof beams, and precast concrete roof slabs. The walls in the Romeoville building are shielded with lightweight wire mesh cast in the panels and bonded to a copper perimeter loop around the foundation. The floor shielding consists of a metal-backed raised floor system. Individual copper conductors in each of the roof rafters provide the roof shielding. The Frankfort building is similar in construction but has additional shielding against low-frequency magnetic fields and high-frequency radiated EM fields.

Table 3-1 shows the results of the measurements obtained in a 1965 study that measured the shielding provided by these two buildings. It is seen that the electric-field attenuation provided by the Romeoville building ranged from 39 dB at 18 kHz to -1.5 dB (an enhancement) at 96 MHz. The attenuation provided by the Frankfort building ranged from 51 dB at 18 kHz to 5 dB at 90 MHz.

Table 3-1. ELECTRIC-FIELD ATTENUATION OF TWO 5ESS PRECAST CONCRETE BUILDING SITES

Location	Frequency	Attenuation
Romeoville, Illinois	18 kHz	39 dB
	890 kHz	27 dB
	1 MHz	21 dB
	96 MHz	-1.5 dB
Frankfort, Illinois	18 kHz	51 dB
	560 kHz	43 dB
	890 kHz	43 dB
	1 MHz	43 dB
	90 MHz	5 dB
	96 MHz	10 dB

We also found that shielding measurements had been made at an underground power-feed building in Beaucoup, Illinois. Because of the underground location, the measurements are probably of marginal interest to us; but it was stated that the poured-in-place structure owes its shielding capability solely to the presence of its wire-tied reinforcing. Thus, the results might be applicable to a single-story, windowless, aboveground structure of similar wall and roof construction. The measurements showed that the building shielding exceeded 25 dB at all frequencies above 50 kHz (with the exception of a 24-dB shielding value at 96 MHz) and exhibited a drop-off of not more than 20 dB per decade below 50 kHz.

We also found documentation on shielding measurements made for three buildings that actually house 5ESS Switches. The first of these was for the building enclosure that houses the 5ESS Switch at Sugar Grove, Illinois. Measurements were made at frequencies between 20 and 220 MHz. The average attenuation in this range was reported to be 24 dB.

The second case is for the building containing the 5ESS Switch at Seneca, Illinois. Wall attenuation levels between 5 and 9 dB were reported, with the wall becoming more transparent at the lower frequencies (below about 40 MHz).

The third case is for a building at Fort Branch, Indiana. This building, made of cement block and brick, showed an attenuation level of about 3 dB at 95 MHz.

The few data available for buildings that actually house 5ESS Switches are summarized in Table 3-2; it is rather obvious that the entries of this table (even when supplemented with those of Table 3-1) are insufficient to derive a frequency-dependent transfer function for building types of interest to this study. We therefore expanded our literature search to see if sufficient work had been done on non-PSN buildings to define a transfer function for relevant PSN buildings of concern in this study. The following material reports on the results of that effort.

Table 3-2. ELECTRIC-FIELD ATTENUATION OF THREE 5ESS™ BUILDING SITES

Location	Average Attenuation
Sugar Grove, Illinois	24 dB in the frequency range from 20 to 220 MHz
Seneca, Illinois	5 to 9 dB
Fort Branch, Indiana	3 dB at 95 MHz

3.2.2 Data for General Building Types. As noted above, since the search for a sufficiently complete data base of measured EM shielding values for PSN buildings proved unsuccessful, we turned our attention to a study of the available literature for information on shielding values for non-PSN buildings.

One of the first things that happened in this effort was a reinforcement of our initial feeling that one *must* have access to valid experimental data if one is to have confidence in the shielding values claimed for a particular building type: an analytical approach is not feasible. The geometry of typical building types is usually very complicated and difficult to model; and frequently there are apertures in the building (such as doors and windows), which further complicate any attempt to determine building shielding factors analytically. Thus, we quickly restricted our endeavors to a search for experimental measurements.

The published literature reports on many measurements of the shielding effectiveness of various building types and constructions. The measurements come from several kinds of studies — electromagnetic compatibility (EMC), electromagnetic interference (EMI), lightning, etc. Much of the experimental work uses ambient radio signals present in the region around a building as sources for the EM radiation needed to determine shielding effectiveness. Unfortunately, these sources are not present at the low-frequency end of the spectrum where the EMP signal has most of its energy.

The bibliography at the end of this document lists many of the reports consulted during this study. Among those, the paper by A. A. Smith (see Reference 2) provides the most comprehensive survey of shielding measurements, presented in a readily usable format. One reason for the usefulness of this paper is that the measured attenuation values are provided for seven individual building types.*

Building Types 1 and 2, single-family detached residences, are not relevant to this study. But Building Types 3 and 4 are single-story, concrete-block structures that are highly representative of the buildings that one would expect to find at rural and small suburban switching locations. In addition, Building Types 5 through 7 are multi-story structures that appear to be representative of PSN buildings that house switching equipment in urban and large suburban installations; the attenuation provided by such buildings is of interest in the overall NCS program. Thus, we elected to utilize the data base presented in the Smith paper to characterize five different structure types deemed representative of relevant PSN buildings, with the two single-story types being of primary interest in the current study effort. The decision to concentrate on the results in the Smith paper was given additional impetus when it was noted that several other papers viewed his results with high esteem (see, for example, Reference 3).

The structural characteristics of the various building types are summarized in the following paragraphs; graphs are included presenting the measured electric-field shielding data reported by Smith. The data were obtained by measuring the field strengths of ambient broadcast signals of opportunity both inside and outside each building and plotting the observed attenuation as a function of frequency. These sources were supplemented by a mobile transmitter capable of generating signals at 7, 21, and 29 MHz to supplement the available broadcast frequencies. The attenuation values were expressed in decibels (dB).

Figures 3-1 and 3-2 present the data reported for the two types of detached, single-family houses. Type 1 represents a house with wood and brick siding, whereas Type 2 is a similar structure with partial aluminum siding. Although these structures are not of any real interest to us in this study, the data do show that the additional metal on the exterior of Building Type 2 has a minimal effect on the attenuation of incident electric fields. This is an important point to remember: although the amount of metal in the exterior of each building type increases as one goes to higher building type

* We use the term "Building Type" in this document to label the various sets of shielding data presented in the Smith paper. In actuality, each such "Building Type" reflects only a single building located in Ulster, Greene, Dutchess, or Albany County of New York. However, the design differences between the various buildings are sufficiently distinct and the construction details of each are sufficiently representative of a large number of commercial buildings to justify our terminology.

number, the increased metal content may not have a marked impact upon the measured shielding effectiveness levels. One important reason for this is that the effects of large apertures can negate the potential shielding effectiveness of the additional metal.

The solid lines in Figures 3-1 and 3-2 represent fifth-degree polynomial fits to the means of the measured data and each point represents the results of a single attenuation measurement. The means of the measured data at a given frequency were calculated from the individual measurements at that frequency, assuming a log-normal distribution of those measurements. A similar interpretation is to be assigned to the graphs for Building Types 3 and 4.

The measurements for Building Type 3 are presented in Figure 3-3. Building Type 3 is a concrete-block structure with a large metal-frame window across the front. The structure is supported with steel columns and a steel-bar joist-supported roof and is erected on a standard reinforced concrete slab on grade. The interior is divided into cubicles with demountable steel and glass partitions. In fact, this type of interior was present in Building Types 3 through 6. Recessed fluorescent fixtures are inset into the suspended ceiling. An extensive but typical array of ducts, pipes, and cables occupies the space above the suspended ceiling.

Figure 3-4 presents the results of measurements for Building Type 4, where the solid line again represents a fifth-degree polynomial fit to the measured means. This building type is very similar to Building Type 3: both are concrete-block, steel-frame buildings erected on a reinforced concrete slab poured on grade. There is more metal in the exterior walls of Building Type 4, however, partly owing to the presence of steel-frame doors and a rather large number of isolated steel-frame windows in the external wall. The larger electric-field attenuation values for Building Type 4 in the frequency range between 1 and 100 MHz, relative to those for Building Type 3, are consistent with the larger metal content of the building.

Building Type 5 is a four-story office building. It has a steel frame with preformed concrete exterior wall panels and continuous aluminum window frames on three sides. The fourth side is covered with metal exterior wall panels and has a continuous floor-to-roof vertical window in the center of the wall. The floors are corrugated steel covered with poured concrete. Figure 3-5 presents the results of the measurements of the electric-field attenuation provided by this building. The graph reflects three departures from the treatment given in Figures 3-1 through 3-4. First, the observed correlation of increased attenuation values with increased distance of the sensing antenna from the outside walls of the building has justified showing four different fits to the data, one for each of the four distances from the outer wall represented in the measured data. Second, a single point in Figure 3-5 represents the *mean* of the individual data measurements at a given frequency and distance from the outer wall, rather than an individual measurement. Third, the number of

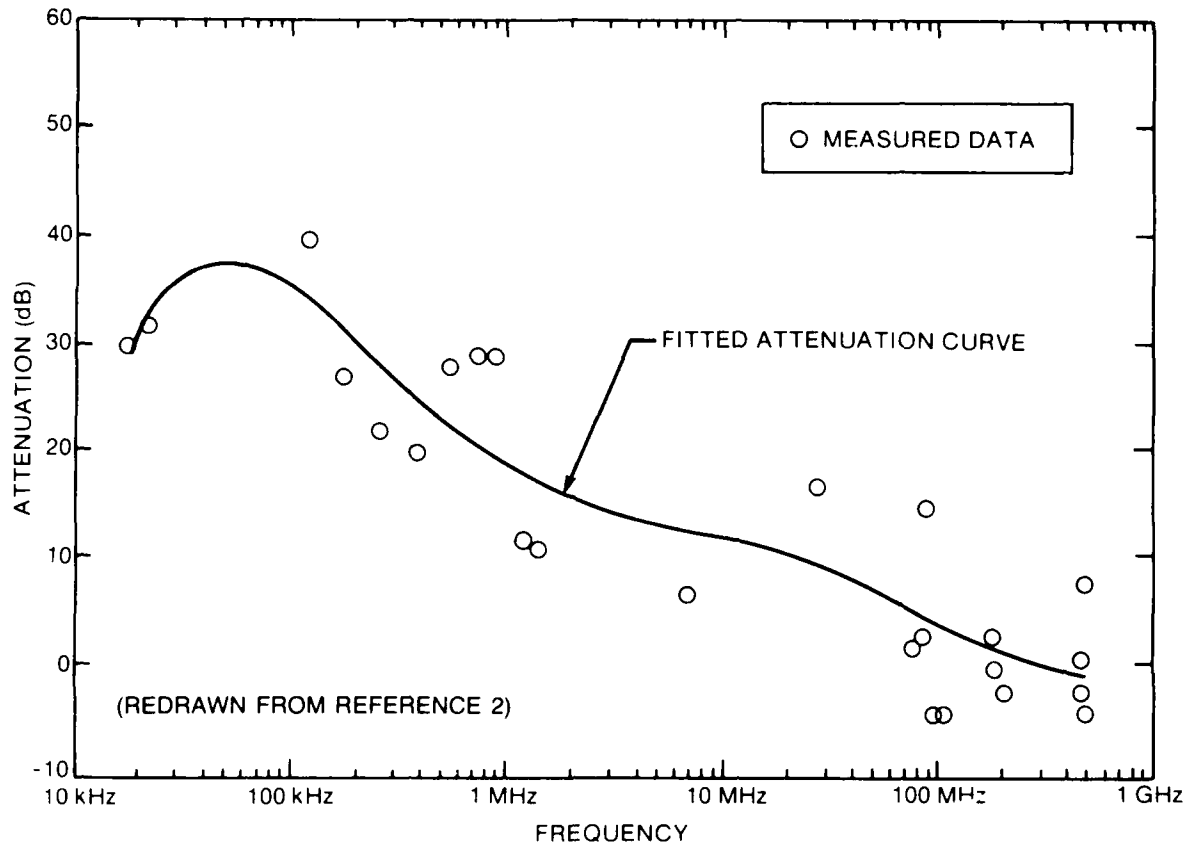


Figure 3-1. Electric-field attenuation — single-family residence with wood and brick siding (Building Type 1).

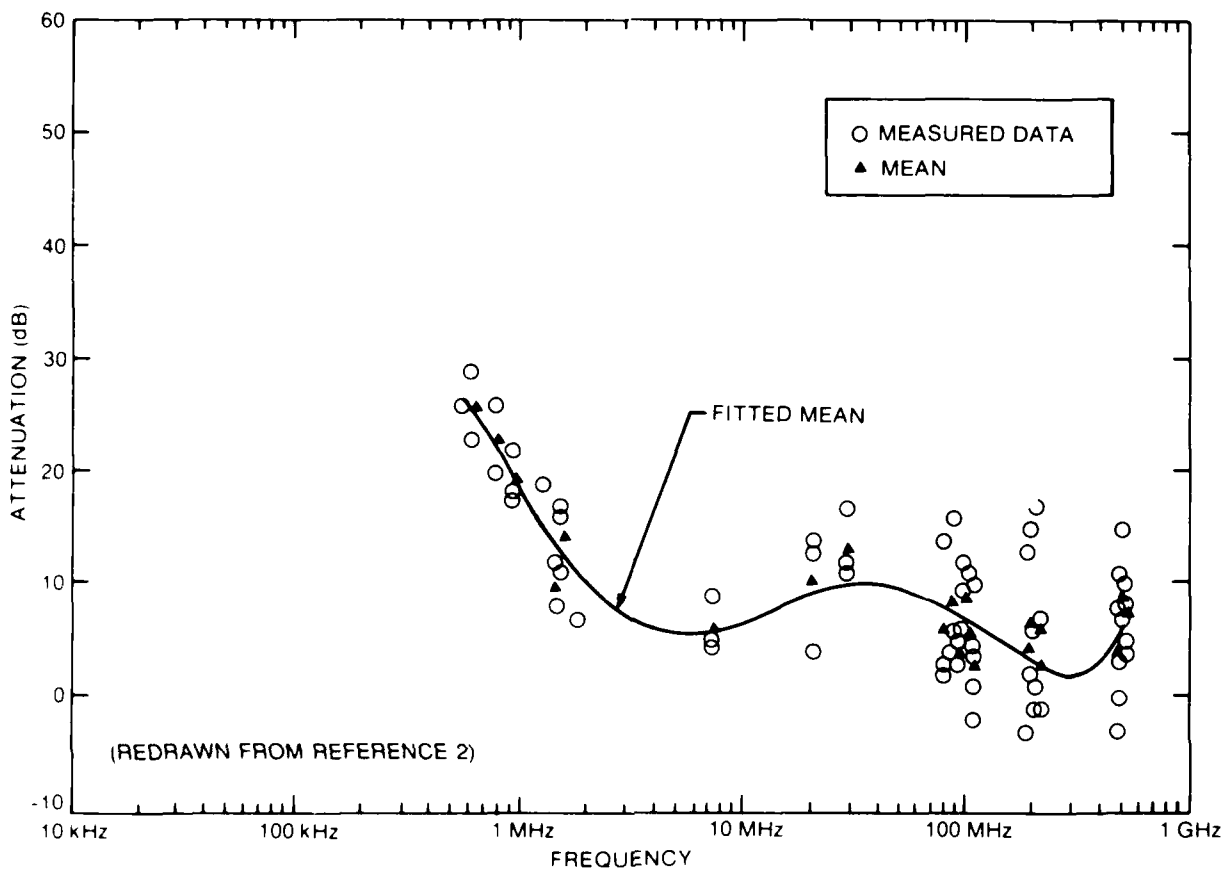


Figure 3-3. Electric-field attenuation — single-story concrete-block building (Building Type 3).

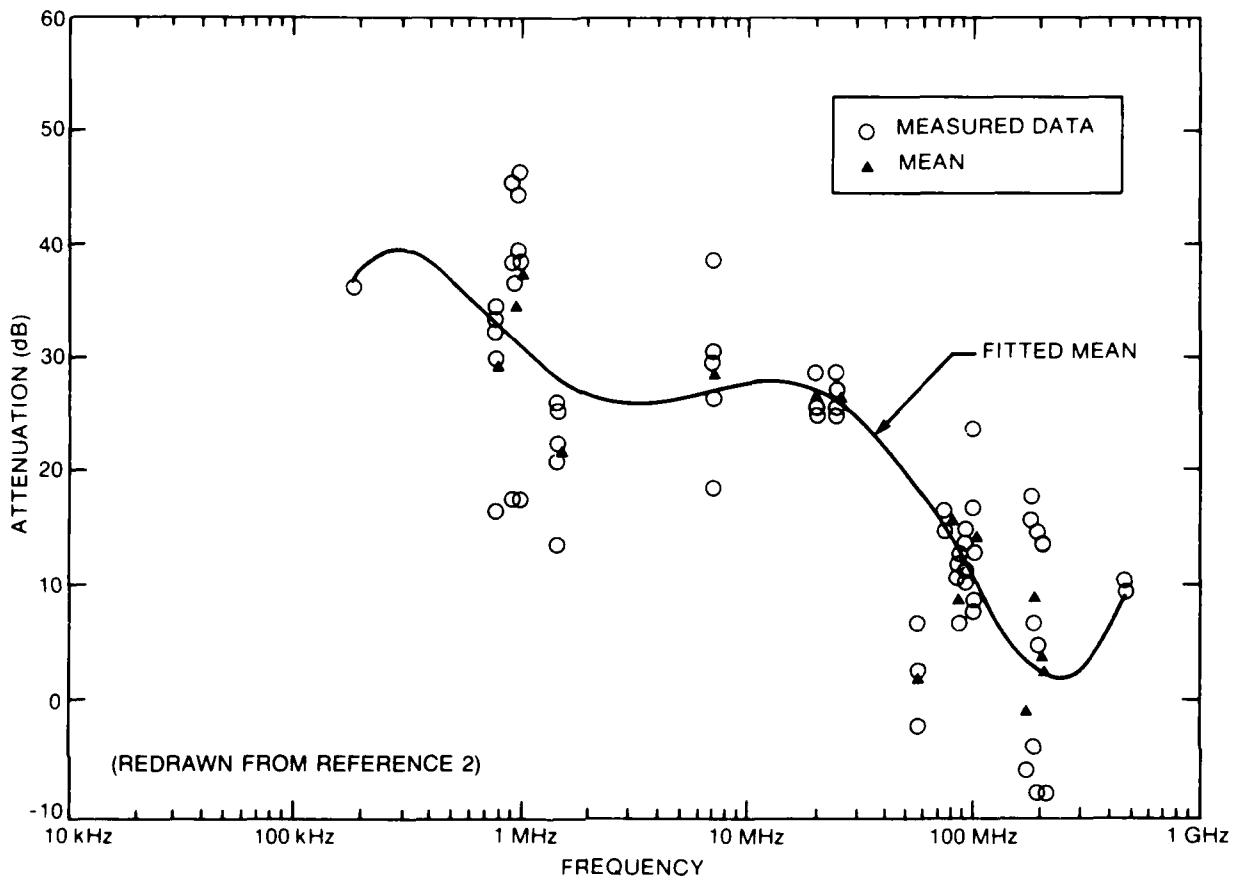


Figure 3-4. Electric-field attenuation — single-story concrete-block building (Building Type 4).

different frequencies represented in the measured data justified using only a third-degree polynomial to fit the means, rather than a fifth-degree expression.

Figure 3-6 presents the results of the measurements on Building Type 6 in a format similar to that used in Figure 3-5. Here, however, the number of frequencies in the data base was deemed sufficient to warrant a fifth-degree polynomial fit. This building type is a four-story office building, just as is Building Type 5, but it has a brick exterior and isolated aluminum frame windows.

The last type of building is a 20-story office building. Building Type 7 is a steel-frame building with marble exterior panels and continuous aluminum-frame windows on all four sides. Interior steel columns are spaced approximately 7 meters apart. The floors are corrugated steel covered with poured concrete. The interior of this building is different from that of any other building type discussed here: it contains only a few interior walls and partitions constructed of non-conducting material. There is a suspended ceiling with recessed fluorescent lighting fixtures on each floor. Electrical wiring is routed in raceways in the floor, and air ducts in the ceiling are flush with the corrugated steel overhead. The measured electric-field attenuation data are presented in Figure 3-7 in a format equivalent to that used for Building Type 6 in Figure 3-6. As is the case for Building Types 5 and 6, this building showed a strong variation in attenuation with distance from the exterior wall.

A number of observations should be made regarding the data shown in the figures presented in this section. First, from Figures 3-3 and 3-4, for which an individual point on the graph represents a single measurement, it is clear that rather large differences exist in the observed attenuation values at different points within the building. This should not be surprising when it is realized that the measurement locations within Building Type 4, for example, spanned the range from 2 to 50 meters from the outside walls. Second, it should be recognized that any transfer function derived from the frequency-dependent fits to the means does not have a clearly defined physical definition. Thus, any transfer function derived from the solid curves of the figures should be viewed as only providing some "typical" shielding effectiveness against EMP-like signals: there may be no point within the building where the field looks like what is calculated from this transfer function, and significant variations from this "typical" value can be expected. This latter observation holds even for Building Types 5, 6, and 7, for which cases the fits have been constrained to measurements taken at a fixed distance from the outer wall: the average standard deviation in the measurements for data taken at a given distance from the wall and a given frequency for Building Type 5 was of the order of 9 dB, according to Smith (Reference 2).

Fourth, even for Building Types 3 and 4, for which a data point on the graph denotes a single measurement, one is unable to construct a transfer function that will produce an attenuated

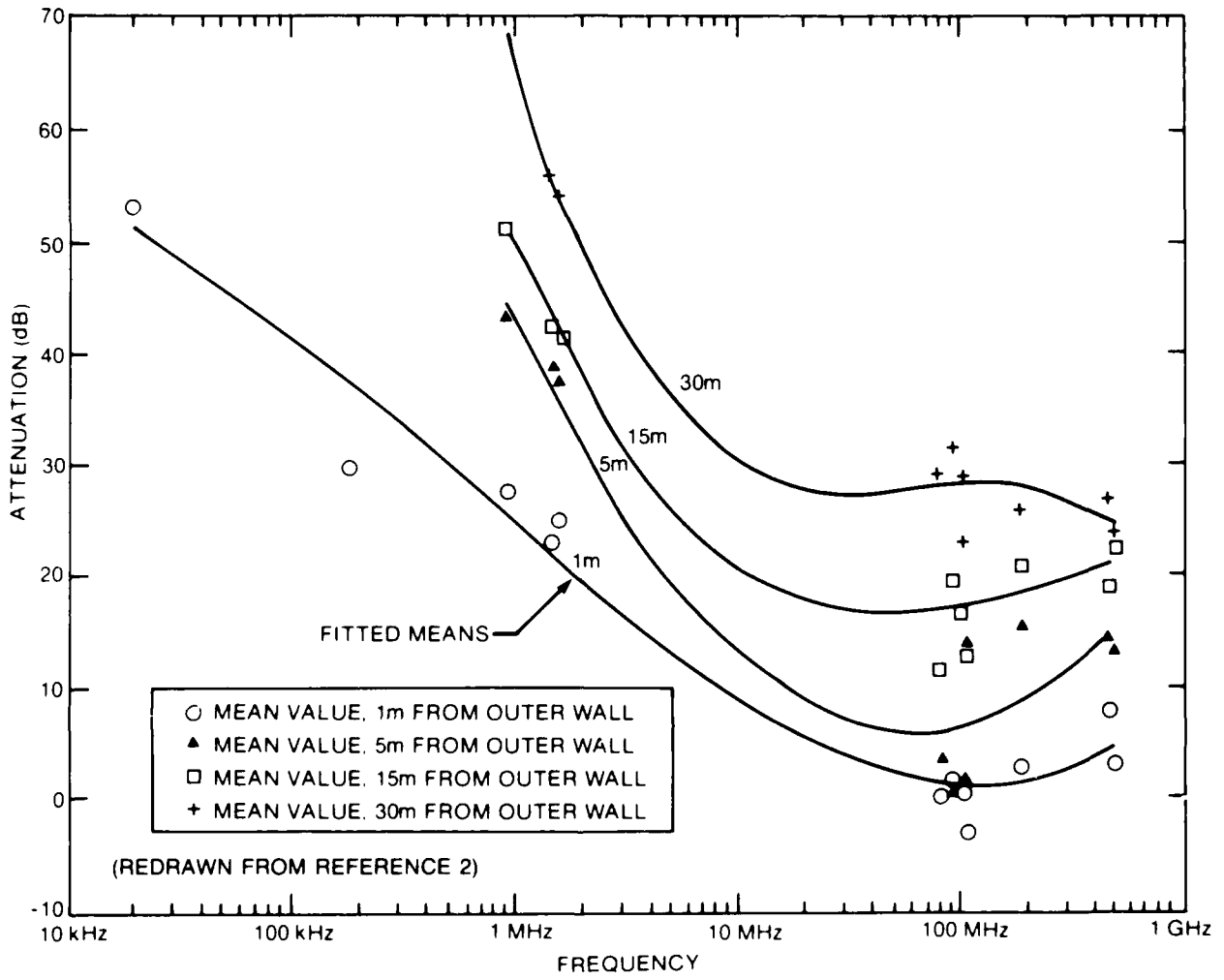


Figure 3-5. Electric-field attenuation — four-story office building (Building Type 5).

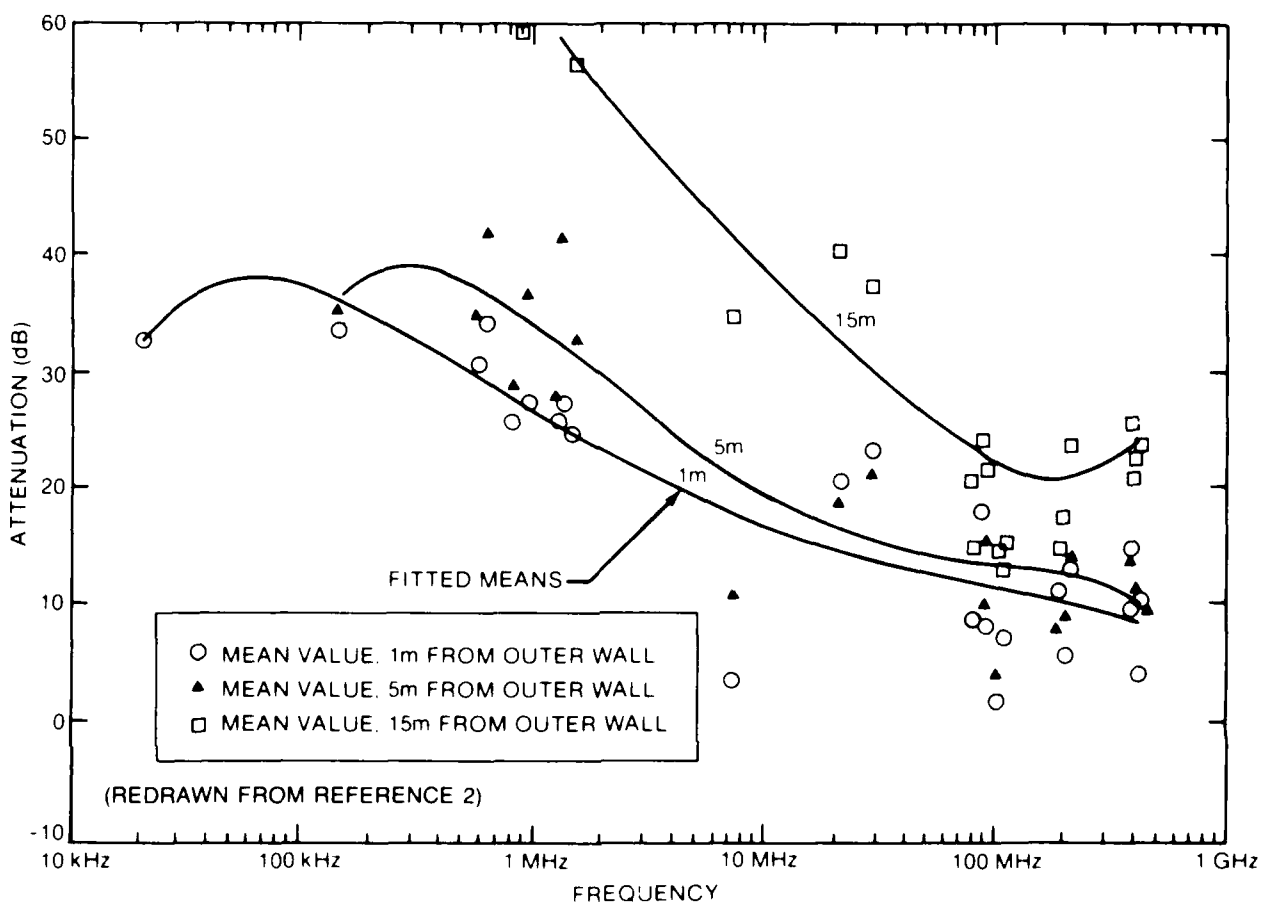


Figure 3-6. Electric-field attenuation — four-story office building (Building Type 6).

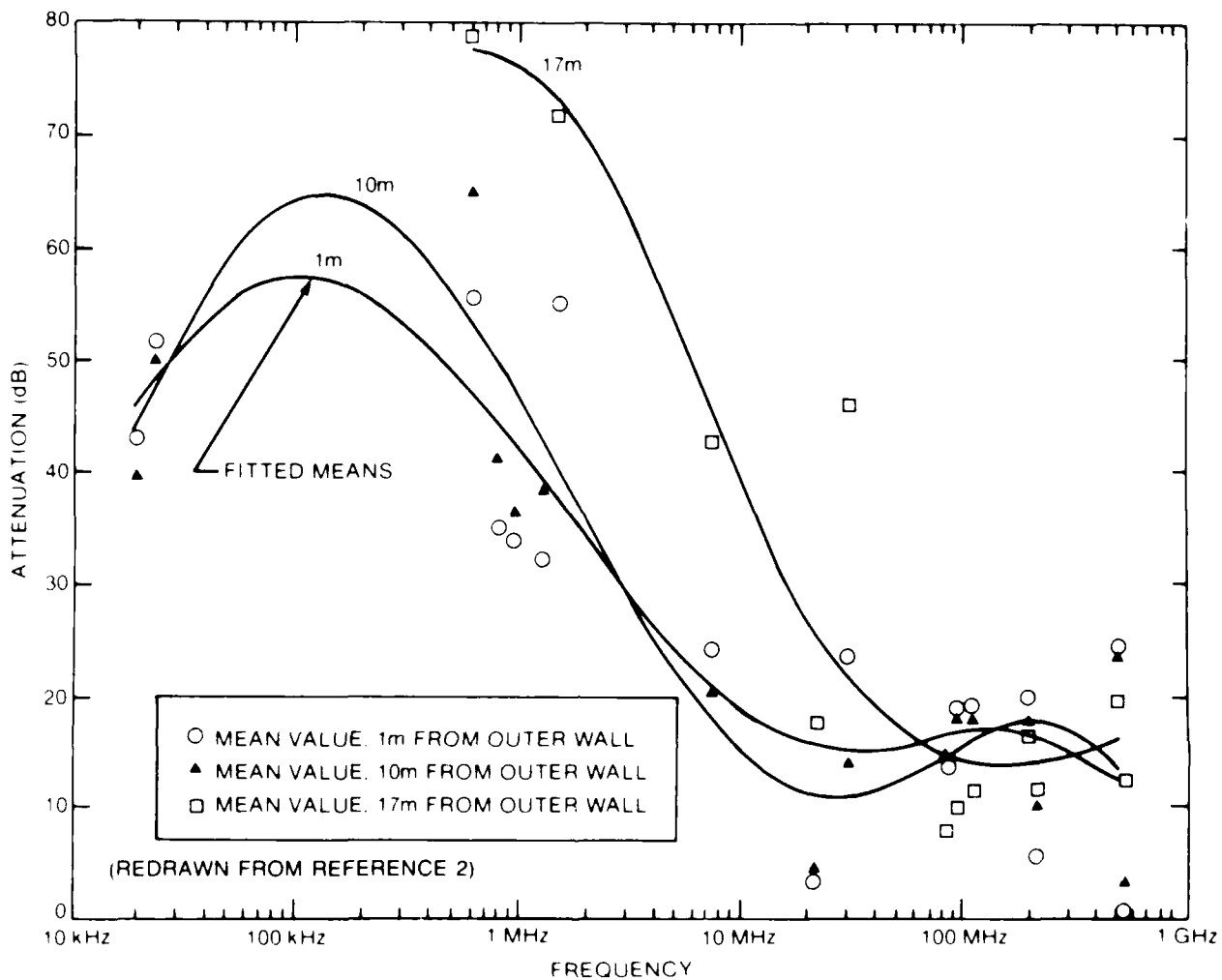


Figure 3-7. Electric-field attenuation — twenty-story office building (Building Type 7).

EMP-like field that is anything more than "typical": the data for the two buildings are not labeled as to measurement point.

Although the building shielding capabilities predicted by the transfer functions derived from the data of Figures 3-3 through 3-7 must be viewed as only "typical," we proceed to a determination of what such transfer functions imply about the magnitude of interior fields and field-induced cable currents when a building is subjected to an incident EMP-like wave. We will point out the limitations that should be placed on the interpretation of the results as we perform the analysis.

3.3 Shielding Effectiveness Calculations

The major purpose of this subsection is to present the results of an effort to construct transfer functions from the data presented on the previous pages and to predict transients expected interior to various types of buildings when illuminated with EMP-like waves. Before discussing the details of that effort, however, let us make a few comments on the nature of the data presented in Section 3.2 and the significance of the transfer functions we have derived from those data.

All building types under consideration have rather significant apertures through which EM energy can penetrate to interior points. Thus, the typical field at any interior point will be made up of a direct component (usually reduced in intensity from that of the wave incident upon the building) and one or more reflected components. Taking this into account, let us make some observations as to the expected nature of shielding measurements on such structures in an attempt to identify the appropriate way to interpret and use the measured data.

To this end, assume that we have a building in which measurements are made of the received power at points where the resultant field is made up of a direct monochromatic CW signal and a single reflected wave. Under these circumstances, measurements of the power received by an antenna at a given location within the building will show alternate minima and maxima as one sweeps across the frequency spectrum, with these extrema being associated with destructive and constructive interference between the direct and reflected signals. For example, measurements taken at a point at which the effective path-length difference for the direct and reflected signals is 9 meters will exhibit a transition from maximum to minimum received power as the frequency goes from 100 MHz (for which case the 9-meter path difference is an integral number of wavelengths) to 116.7 MHz (at which frequency the 9-meter path difference is a half-integral number of wavelengths).

It should be noted, however, that if one now makes measurements at a second interior point, the frequencies at which local extrema occur will in general be shifted from those observed for the original measurement location. Thus, if we plot the relative received power for a number of observation locations as a function of the (monochromatic) frequency of an incident CW signal, the

aggregate data will form a band of data points extending across the frequency range. One edge of the band represents the received power under conditions of destructive interference; the other, constructive interference.

The original data for a single measurement location would, in principle, permit one to construct an attenuation function to describe the time-dependent field at that point within the building when the building is subjected to an EMP-like wave that contains significant energy over a wide frequency range. But if one were presented with only the aggregate plot of all CW data points (the band of points described above), such a reconstruction would not be possible, since the data points for a single measurement location are neither all at the top nor all at the bottom of the band: the data points for a single measurement location oscillate between the top and bottom of the band as one sweeps through frequency.

Note that the data of Figures 3-3 and 3-4 present us with a dilemma similar to that presented above. We have a wide band of data representing measurements taken at a large number of points, but we do not know which data points came from a given measurement location. As noted above, we will not be able, therefore, to construct a transfer function to describe the interior field resulting from an incident EMP-like wave at an arbitrary point in the building. But there are a few observations that can be made concerning use of the aggregate data for the simplified case outlined above that should also be valid for our attempts to make meaningful use of the data presented in the previous section for measurements on complex structures.

- First, the power received at any interior point will be less than that calculated on the basis of a transfer function derived from the data points at the bottom of the data band (i.e., for data points associated with minimum power loss).
- Second, the energy received at any interior point will be greater than that calculated from the points on the upper edge of the band.
- Third, the actual transfer function for any one location will in general be different from that for another (otherwise, the spread in data points would not be present).
- Fourth, therefore, although a transfer function calculated from the mean of the data points does not represent a physically realizable situation (since no single point would exhibit the shielding values of the means), such a function will support the derivation of frequency-domain descriptions of interior fields that have total and frequency-dependent energy contents truly typical of actual fields. (In fact, for the simple case described above where we have only a direct wave plus a single reflected wave, the frequency-dependent energy spectrum can be shown to be given exactly by the transfer function derived from using the mean data points, for an appropriately defined mean.)

- Fifth, although a given energy spectrum does not uniquely define a time-domain signal, the time-domain signal predicted on the basis of the transfer function derived from the mean of the data points can be viewed as "typical."

With the above points in mind, we proceeded to utilize the mean-data fits of Reference 2 to derive fits to complex transfer functions for the five building types of interest. To accomplish this task, however, it was necessary to extend the data to low frequencies not represented in the measurements. Such a step was needed to give reasonable behavior to the transfer function in regions where the incident EMP-like waves have an appreciable part of their energy. This was done by insisting that each transfer function not only reproduce the mean data curves of Reference 2, but also describe a shielding effectiveness that smoothly approaches some asymptotic value as the frequency goes to zero. Table 3-3 shows the selections made for this study, where the values shown are the low-frequency asymptotes for the shielding attenuation, given by

$$20 \log | a_{\text{bldg}}(\omega) | .$$

The reader will note that values are given in this table for three different cases for Building Type 3: one for minimum attenuation, one for the mean attenuation, and one for maximum attenuation. The minimum- and maximum-attenuation cases are included because we wished to determine what we would find if we used the extreme, rather than the mean, of the measured data in predicting internal transients resulting from illumination of buildings by EMP-like waves. The minimum- and maximum-attenuation transfer functions were obtained by fitting the upper and lower envelopes that bound the measured data points. For example, we drew a line connecting the topmost points of Figure 3-3 and constructed an analytic complex transfer function consistent with these data for the maximum-attenuation case. We elected to carry these three cases for Building Type 3 all the way through our analysis in order to get a quantitative estimate of the differences that would appear in the energy content and time-domain signals for the absolute extreme cases reflected in the data (recognizing, as pointed out previously, the energy content of physically realizable signals will never be as large or small as predicted by these extreme data).

We also include in Table 3-3 an entry for the trailer used to house the switch tested at AFWL. We include the tabular entries for that structure in this section so that the reader can compare the shielding predicted for the trailer with what we predict for the various building types.

Using the low-frequency asymptotes of Table 3-3, we then fit the data of Figures 3-3 through 3-7, noting that what is plotted on these figures is given by

$$-20 \log | a_{\text{bldg}}(\omega) | .$$

Table 3-3. ASYMPTOTIC SHIELDING ATTENUATION VALUES USED IN FITTING ANALYSIS (AT LOW FREQUENCIES)

Building Type	Asymptotic Value (dB)
3 (min attn)	-30
3 (mean attn)	-42
3 (max attn)	-42
4	-46
5 (1 meter inside)	-50
5 (5 meters inside)	-66
5 (15 meters inside)	-74
5 (30 meters inside)	-80
6 (1 meter inside)	-40
6 (15 meters inside)	-60
7 (1 meter inside)	-54
7 (17 meters inside)	-80
Test Trailer	0

The analytic fits for the various $a_{\text{bldg}}(\omega)$ were then used to calculate the time-domain fields seen within various buildings for cases when an EMP-like field was incident on those buildings. The incident fields used for this exercise were the single- and double-exponential fields defined earlier, in Section 2 of this report. The resulting peak values of the interior electric fields are shown in Table 3-4, where the interior field strength is expressed in dB relative to the incident field strength. The table also shows the relative energy content of the interior fields predicted from our analytic fits to $a_{\text{bldg}}(\omega)$.

A comparison of the three entries for Building Type 3 shows that a 6-dB difference in interior-field energy is associated with the extremes of the data in Figure 3-3. However, as we pointed out, the energy actually present at a given location will lie somewhere in between these two extremes; i.e., near to that predicted by the mean data. But even if the internal electric-field energy levels actually assumed these extreme values at some points, one could still say that the energy content of the field at any interior point is within about 3 dB of that predicted from the mean data. This factor-of-two uncertainty is, perhaps somewhat larger than one would like to be able to cite for a building; but the accuracy is somewhat better than one would estimate initially from looking at the data of Figure 3-3.

A similar set of considerations can be made concerning the possible spread in peak electric-field values: we fully expect that the spread in actual peak field strengths seen inside Building Type 3 will be less than the 18-dB difference derived from the minimum- and maximum-attenuation envelopes

Table 3-4. INTERNAL ELECTRIC FIELDS FOR VARIOUS BUILDING TYPES (NO FLOOR/GROUND REFLECTIONS)

Building Type	N_{exp} *	Max. E-Field (dB)†	Energy Content (dB)†
None	1	0	0
	2	0	0
3 (min attn)	1	+2.3	-10.1
	2	-0.4	-10.7
3 (mean attn)	1	-9.0	-13.8
	2	-12.0	-14.0
3 (max attn)	1	-16.4	-19.1
	2	-17.0	-19.1
4	1	-9.3	-27.3
	2	-16.8	-29.9
5 (1 meter inside)	1	-2.2	-17.8
	2	-6.0	-19.0
5 (5 meters inside)	1	-9.9	-21.7
	2	-10.9	-22.4
5 (15 meters inside)	1	-18.9	-31.1
	2	-20.5	-31.8
5 (30 meters inside)	1	-28.4	-40.6
	2	-30.0	-41.3
6 (1 meter inside)	1	-10.7	-24.0
	2	-15.7	-24.5
6 (15 meters inside)	1	-23.3	-43.3
	2	-30.3	-46.4
7 (1 meter inside)	1	-14.5	-24.0
	2	-18.4	-24.5
7 (17 meters inside)	1	-17.5	-43.3
	2	-24.8	-46.4
Test Trailer	1	+0.01	+0.01
	2	+0.04	+0.008

* $N_{exp} = 1$ for single-exponential field; $N_{exp} = 2$ for double-exponential field.

† Relative to value for appropriate driving field in absence of building.

of Figure 3-3 (see the discussion at the beginning of this section). There are some applications for which this factor-of-three uncertainty about some nominal value of the peak electric-field amplitude will be acceptable; for others, not. We comment further on this point in Section 4.

A cursory look at the spread of the data in Figure 3-4 seems to indicate that a similar spread in peak-field and field-energy values would be obtained if we were to subject the data of Building Type 4 to the same kind of analysis.

It was postulated that much of the spread in the measured attenuation data for Building Types 3 and 4 was due to the fact that the data at a given frequency represented measurements taken at a number of interior points. Such was, indeed, the case; and, therefore, it might be hoped that the categorization of the data by the distance of an observation point from the exterior walls of a building would reduce the spread associated with each category of attenuation data presented for Buildings 5, 6, and 7. However, based on the discussion of Reference 2, it appears that an average standard deviation of slightly over 9 dB should be associated with the measurements taken a fixed distance from the exterior walls of Building Type 5, with a range in these standard deviations from 0.5 to 19 dB. Thus, it would appear reasonable to state that, at any arbitrary point within Building Types 3 through 7, nominal peak-field and field-energy values to be associated with an EMP-like field can be derived from the mean data fits, but extreme values may occur that differ from these nominal ones by a factor of two or three.

Therefore, if we wish to assign a value to the peak electric field or electric-field energy content at an interior point of Building Type 3 or 4, we would ordinarily use the value computed from the mean-data fits of Reference 2 and note that an uncertainty factor of two or three should be associated with that nominal value. Since the mean-data fits were obtained from measurements obtained throughout the interior of these two building types, such an approach is, *a priori*, appropriate for any interior point. However, it is reasonable to assume that points near the outer wall of such a building type will exhibit field strengths and energy levels skewed to the high side of the nominal value, and that points deep within such buildings will exhibit values skewed to the low side. Such a situation is expected and is fully consistent with the results for Building Types 5 through 7, for which we are able to derive a number of so-called nominal field values, each being associated with a given distance from the outer building walls.

Characterization of the interior fields in terms of their energy content and peak amplitudes is certainly indicative of the relative effect of these fields on equipment inside a building. However, a more meaningful measure of the impact of an interior field is the magnitude of the cable current that such a field will generate. Thus, we calculated the peak cable currents that the predicted interior fields would induce. These calculations were done for three cable lengths: 1, 10, and 50 meters. The incident external field was assumed to have its electric vector aligned parallel to the

cable, and each cable was assumed to be shorted. Currents were calculated using the formalism summarized in Appendix B, which contains material taken from Reference 1.

Although some cable-current calculations were made in the absence of reflections of the driving fields off the floors of the buildings, most of the predictions were made for the case of an imperfectly reflecting floor located two meters below each exposed cable. The incident field was assumed to have a propagation vector 30 degrees from the vertical, and the floor was assigned a conductivity of 0.01 mho/meter. Table 3-5 presents the peak electric field strengths of the internal fields (as seen by the cables) for this set of circumstances. In each case, the peak field was not very different from that listed in Table 3-4 for the case when there is no reflection from the floor. It should be recognized, however, that the late-time behavior of the fields is quite different in the two cases: the interference of the reflected wave with the direct field produces a rapid decrease in the resultant field after the arrival of the reflected wave from the floor.

Table 3-6 shows our predictions for the peak currents induced on the cables for an incident external field of 1 kV/meter. We express these peak current values in dB, relative to the values predicted in the absence of the buildings. Several characteristics can be identified from a study of this table and the entries of Tables 3-4 and 3-5.

- First, the peak currents expected on short cables are extremely well correlated with the peak electric-field-strength values. This is expected, since the currents on a short cable are expected to follow the time behavior of the driving field as long as the field stays at near-peak levels for at least a nanosecond.
- Second, the peak currents predicted for the longer cables show a similar correlation, but with an important difference: whereas the peak currents on the short cables are proportional to the predicted peak electric field values, the peak values for the longer cables are somewhat smaller inside a building (relative to the case where the building provides no attenuation) than such scaling would predict. This is understandable in view of the fact that the buildings are better attenuators of low-frequency than of high-frequency signals and the lower frequencies make significant contributions to the currents on these cables. The only exception to this general observation is for the case of a 10-meter cable inside Building Type 3, where its peak current is predicted to be significantly larger than even that which would be predicted on the basis of peak-field scaling. It turns out, however, that the driving field for this particular case is unusual in that, owing to early phase reversals of the field, the reflected-plus-direct field resultant persists at a significant strength for tens of nanoseconds after arrival of the reflected wave.
- Third, in view of the above points, we conclude that the uncertainty in predicted cable currents above a reflecting floor will be of the same magnitude as the uncertainties in the peak electric field: about a factor of two or three in amplitude.

Table 3-5. PEAK INTERNAL ELECTRIC FIELDS FOR VARIOUS BUILDING TYPES AT A HEIGHT OF 2 METERS ABOVE REFLECTING FLOOR/GROUND WITH $\sigma = 0.01$ MHO/METER

Building Type	N_{exp} *	Max. E-Field (dB)†
None	1	0
	2	0
3 (min attn)	1	+3.0
	2	-0.2
3(mean attn)	1	-9.7
	2	-10.1
3 (max attn)	1	-16.1
	2	-16.4
4	1	-10.0
	2	-16.4
5 (1 meter inside)	1	-1.4
	2	-5.7
5 (5 meters inside)	1	-8.4
	2	-9.3
5 (15 meters inside)	1	-18.4
	2	-
5 (30 meters inside)	1	-27.9
	2	-
6 (1 meter inside)	1	-9.5
	2	-
6 (15 meters inside)	1	-21.8
	2	-
7 (1 meter inside)	1	-15.3
	2	-
7 (17 meters inside)	1	-16.0
	2	-
Test Trailer	1	-2.0
	2	-1.4

* $N_{exp} = 1$ for single-exponential field; $N_{exp} = 2$ for double-exponential field.

† Relative to peak field for appropriate driving field in absence of building.

Table 3-6. PEAK CURRENTS ON CABLES 2 METERS ABOVE FLOOR FOR 1-KV/METER INCIDENT FIELDS ($\sigma = 0.01$ MHO/METER)

Building Type	N_{exp} †	Max Current (dB)* for Cable Length of		
		1 meter	10 meters	50 meters
None	1	0	0	0
	2	0	0	0
3 (min attn)	1	+3.2	-3.3	-5.5
	2	+3.0	-3.7	-4.9
3 (mean attn)	1	-9.1	-5.8	-10.5
	2	-9.1	-5.7	-10.5
3 (max attn)	1	-15.8	-10.6	-15.6
	2	-15.9	-10.4	-15.6
4	1	-14.7	-20.2	-26.5
	2	-15.3	-22.3	-27.1
5 (1 meter inside)	1	-1.7	-8.2	-11.5
	2	-2.0	-8.0	-12.0
5 (5 meters inside)	1	-7.4	-10.3	-14.3
	2	-6.1	-11.1	-15.1
5 (15 meters inside)	1	-17.7	-18.3	-24.0
	2	-	-	-
5 (30 meters inside)	1	-27.2	-27.9	-33.5
	2	-	-	-
6 (1 meter inside)	1	-12.3	-18.7	-19.5
	2	-	-	-
6 (15 meters inside)	1	-26.3	-33.2	-38.6
	2	-	-	-
7 (1 meter inside)	1	-16.0	-17.5	-21.3
	2	-	-	-
7 (17 meters inside)	1	-17.0	-29.7	-36.7
	2	-	-	-
Test Trailer	1	-1.9	+0.03	+0.2
	2	-2.0	+0.06	+0.14

* Relative to peak current on given length cable subjected to appropriate incident field in absence of building.

† $N_{exp} = 1$ for single-exponential field; $N_{exp} = 2$ for double-exponential field.

We also made calculations of expected peak currents in shorted cables when the floor was perfectly reflecting and when it was completely non-reflecting. In the former case, the results were quite similar to those shown in Table 3-6 for an imperfectly reflecting floor, except that the enhanced reflected wave generated a sharper cutoff to the resultant wave seen by the cables, thereby reducing the peak currents seen on the long cables to values very nearly those predicted for the short cables. For the no-reflection case, however, results were quite different in two rather significant aspects. First, the lack of a reflected wave off the floor permitted the driving field to act for a much longer time; thus, the peak currents on the 10- and 50-meter cables were significantly higher than shown in Table 3-6. The entries of Table 3-7 show how large an effect this is. Second, the presence of a building caused a much larger decrease in the peak currents predicted for the longer cables than shown in Table 3-6. In fact, the reduction in predicted peak cable current for the 50-meter cable in this case was nearly as large as the predicted decrease in total field energy shown in Table 3-4. Such behavior is not unexpected for the no-reflection case in view of the large attenuation provided by the buildings to the low-frequency components of the incident signal.

Table 3-7. PEAK CURRENTS PREDICTED FOR CABLES 2 METERS ABOVE FLOOR/GROUND IN ABSENCE OF BUILDINGS (1-KV/METER INCIDENT FIELD)

Case	N_{exp}	Peak Current (Amps) for Cable Length of		
		1 meter	10 meters	50 meters
Non-reflecting floor/ground	1	2.63	25	105
	2	1.68	25	103
Perfectly reflecting floor/ground	1	5.2	5.7	5.5
	2	3.2	5.6	5.4
Reflecting floor/ground with $\sigma=0.01$ mho/meter	1	4.0	9.5	12.0
	2	2.63	9.3	12.0

* $N_{exp} = 1$ for single-exponential field; $N_{exp} = 2$ for double-exponential field.

The observations made in the above paragraphs are summarized in Section 4, following, where the significance of the results is also discussed.

4. SUMMARY AND CONCLUSIONS

In order to determine the threat-level transients expected on the various cables of operational 5ESS switches from a knowledge of the transients measured at AFWL for a small switch housed in a fiberglass-clad trailer, it is necessary to know the attenuation afforded by the trailer to the simulated-EMP fields at AFWL and the shielding against threat-level EMP fields provided by the buildings that contain operational switches. This report documents our efforts to determine the appropriate trailer and building attenuation factors.

Using the CW EM-shielding measurements made on the empty trailer, we have found that the effect of the trailer was negligible for incident fields of interest. We found that the peak electric field strength inside the trailer was probably within 2 dB of the peak value of an incident EMP-like wave, whereas the energy content of such a wave is essentially unaffected by the trailer. The trailer appeared transparent to incident magnetic fields. The decrease in peak electric field strength was responsible for the ~ 2 -dB maximum decrease in peak cable current predicted for short (1-meter) cables inside the trailer (relative to the peak currents predicted for cables exposed directly to the incident fields). However, for longer cables, the trailer was predicted to have essentially no effect on the magnitude of the induced cable currents. Thus, we concluded that the presence of the trailer can be ignored, for all practical purposes, in the exercise of extrapolating the test results from AFWL to a 5ESS switch in an operational setting.

Examination and analysis of the available data base characterizing the EM shielding capability of the various types of buildings that can be used to house operational 5ESS switches confirmed a number of observations. First, a wide range of shielding effectiveness is exhibited by the building types of interest. Second, the electric-field attenuation provided by the various types of buildings is smaller at high frequencies than at low frequencies; thus, the peak currents on short cables inside a building exhibit a smaller decrease (from the values associated with direct illumination by the external fields) than do the peak currents on long cables. Third, the energy content and peak electric field strength of the transmitted wave will vary from one point to another inside a building. Variations of a factor of two or three from nominal values were deemed possible, where such nominal values were computed for points anywhere within single-story buildings and for points a given distance from the outside walls for multi-story buildings. Since, in a typical installation, the racks and cabling associated with an operational 5ESS switch are not necessarily constrained to a well-localized part of the building, the exercise to predict transients on the various cables in and leading to the switch will yield only approximate results in the absence of additional field measurements.

Obviously, the difficulty pointed out in the third of the above points would not exist *if* the current data base enabled one to associate an unambiguous internal field with the various locations inside a

building that contains a *SESS* switch. Unfortunately, however, the published data base will not support such a capability. There are several reasons for this, among which are the following:

- For single-story buildings, data are given showing attenuation values at a given frequency for a number of locations within the building. However, the location of the measurement site is not provided for each of the data points shown. Thus, since the data at a given frequency exhibit as much as a 20-dB spread and can (for Building Type 4) represent measurements taken from locations all the way from 2 to 50 meters away from the outer building walls, the determination of an unambiguous frequency-dependent transfer function for specific points within the building is not possible.
- For multi-story buildings, a single data point represents, for a given frequency, the mean of all measurements taken at locations a fixed distance from the outer building walls. However, the number of individual measurement locations associated with a single data point and the spread observed in the attenuation values at these locations are not provided. In addition, Reference 2 reports that a large spread in measured attenuation values is associated with many of the mean data points for Building Type 5. Thus, we concluded that even the multi-story building data are insufficient to define unambiguous transfer functions at points within the structure, even though the published data *are* labeled with the distance of the measurement locations from the external walls.

In spite of the above comments, it *is* felt that data now available *can* be used to define frequency-dependent transfer functions that provide insight into the amount of EM shielding provided by the various building types. These functions can then be used to define "typical" cable currents expected within the buildings. Thus, for example, we conclude that short (1-meter) cables within a single-story building would have peak currents about equal to those induced by the external field if the cables were located right in front of a window; but these currents would decrease by as much as 10 to 15 dB at points well away from the building walls. For long cables of the order of 50 meters in length located well inside such a building, the cable would experience a decrease of some 15 to 30 dB in peak current, relative to that induced by the external field. A smaller decrease of some 5 dB might be expected for such long cables located adjacent to the walls of a single-story building. These conclusions and similar ones for multi-story buildings are summarized in Table 4-1.

In brief, therefore, we have found that the trailer used to house the test unit at AFWL had minimal effect upon the incident fields. The small *SESS* switch was essentially exposed to the free-field drivers generated by the EMP simulators. On the other hand, we were not able to derive unambiguous frequency-dependent transfer functions to support a high-confidence determination of transients for operational switches exposed to threat-level fields. Only a range of possible shielding-effectiveness values could be obtained (see Table 4-1). However, for this program, our inability to determine these transfer functions to any better extent is not as serious as it might be: the results of

the testing discussed in Volume III of this Final Technical Report show that the behavior of the switch is somewhat insensitive to transient level over the range associated with the single-story-building entries of Table 4-1. It is still recommended, however, that additional shielding measurements be taken at several central offices to provide a better data base for the prediction of transients within PSN buildings, particularly since other elements of the PSN may not show such insensitivity to the range of threat-level transients consistent with the entries of Table 4-1.

Table 4-1. EFFECTS OF BUILDING SHIELDING FACTORS ON PEAK CABLE CURRENTS

Case	Decrease in Peak Current	
	1-Meter Cable	50-Meter Cable
Single-story building, next to window/outer wall	0 dB	5 dB
Single-story building, deep interior location	10-15 dB	15-30 dB
Multi-story building, next to window/outer wall	0-10 dB	10-20 dB
Multi-story building, deep interior location	15-30 dB	20-40 dB

REFERENCES

1. "Nuclear Effects Hardening of Call Control Module (CCM) to be Used in the Nationwide Emergency Telecommunications System (NETS), Volume I; Phase I EMP Test Report," Technical Information Bulletin 86-1, National Communications System, January 1986.
2. A. A. Smith, Jr., "Attenuation of Electric and Magnetic Fields by Buildings," IEEE Trans. Electromagnetic Compatibility, Vol. EMC-20, No. 3, August 1978, pp. 411-418.
3. F. Kolmacka, "Attenuation of the Electromagnetic Field by Buildings," Sdelovaci Tech. 28 (4): 1356-6 (1980).

BIBLIOGRAPHY

1. M. Campi, "Survey and Review of Building Shielding to Electro-magnetic Waves from EMP," HDL-TM-78-23, AD-B034726, Nov. 1978.
2. A. Castenot and B. Jecko, "Pénétration d'impulsions électromagnétiques à l'intérieur des bâtiments en béton armé," *Ann. Télécommunications*, Vol. 39, No. 9-10, 1984, pp. 447-456.
3. D. C. Cox, R. R. Murray, and A. W. Norris, "800-MHz Attenuation In and Around Suburban Houses," *AT & T Bell Lab. Tech. J.*, Vol. 63, No. 6, July-Aug. 1984.
4. M. J. Crisp and R. L. A. Goodings, "Electromagnetic Compatibility Within a Broadcast Studio Complex," *IEEE Int. Broadcast Convention*, Sept. 20-23, 1980, pp. 340-343.
5. H. W. Denny, L. D. Holland, S. L. Robinette, and J. A. Woody, "Grounding, Bonding, and Shielding Practices and Procedures for Electronic Equipments and Facilities; Volume 1 — Fundamental Considerations," DOT Report No. FAA-RD-75-215, I, Contract DOT-FA72WA-2850, Chapter 5, Dec. 1975.
6. P. B. Engh, "Experience with the 150 Mc/s Washington, D. C. Bellboy System," *IEEE Trans. Vehicular Communications*, March 1966, pp. 30-36.
7. M. Heddebaut, P. Degauque, and Demoulin, "Approche expérimentale de l'efficacité de blindage des bâtiments de télécommunications," *Ann. Télécommunications*, Vol. 39, No. 9-10, 1984, pp. 457-464.
8. H. H. Hoffman and D. C. Cox, "Attenuation of 900 MHz Radio Waves Propagating into a Metal Building," *IEEE Trans. Antennas and Propagation*, Vol. AP-30, No. 4, July 1982, pp. 808-811.
9. W. Jarva, "Shielding Efficiency Calculation Methods for Screening, Waveguide Ventilation Panels, and Other Perforated Electromagnetic Shields," *Proc. Seventh Conf. on Radio Interference Reduction and Electronic Compatibility*, Nov. 1961, pp. 478-498.
10. F. Kolmacka, "Attenuation of the Electromagnetic Field by Buildings," *Sdelovaci Tech.* 28(4): 1356-6 (1980).
11. Yu. I. Leshchanskii and N. V. Ul'yanychev, "Computation of Dielectric Characteristics for Brick and Concrete with Varying Moisture Content," *Defektoskopiya* (Moscow Inst. of Physics and Tech.), No. 7, pp. 34-39, July 1980.
12. M. T. Ma and M. G. Arthur, "A Study of the Electromagnetic Fields Distribution Inside Buildings With Apertures Excited by an External Source," National Bureau of Standards Report No. NBSIR 82-1659, Feb. 1982.

13. J. T. Milek, "Radio-Frequency Shielding Materials Survey and Data Compilation," EPIC Interim Report No. IR-41, AD735622, Oct. 1970.
14. J. R. Miletta, "Communication Facility Design Practices for Protection Against High-Altitude Electromagnetic Pulse," HDL-SR-83-14, July 1984.
15. S. Mir and D. R. J. White, "Building Attenuation and the Impact on Product Susceptibility," **IEEE 1974 International EMC Symposium Record**, Cat. No. 74CH0803-7-EMC, July 16-18, pp. 76-84.
16. L. P. Rice, "Radio Transmission into Buildings," **BSTJ**, Jan. 1959, pp. 197-210.
17. A. A. Smith, Jr., "Attenuation of Electric and Magnetic Fields by Buildings," **IEEE Trans. Electromagnetic Compatibility**, Vol. EMC-20, No. 3, Aug. 1978, pp. 411-418.
18. T. Takizawa, "Reduction of Ghost Signal by Use of Magnetic Absorbing Material on Walls," **IEEE Trans. on Broadcasting**, Vol. BC-25, No. 4, Dec. 1979, pp. 143-146.
19. E. H. Walker, "Penetration of Radio Signals Into Buildings in the Cellular Radio Environment," **BSTJ**, Vol. 62, No. 9, Nov. 1983, pp. 2719-2734.

APPENDIX A

ANALYTIC FITTING APPROACH

Consider an electric field that is zero for time $t < 0$ and is real for times $t > 0$. Let this field, $E_o(t)$, be incident upon a structure and let the internal field be denoted by $E_i(t)$. We define the Fourier transform (FT) of the incident field by the usual expression

$$\tilde{E}_o(\omega) = \int_0^{\infty} E_o(t) e^{i\omega t} dt, \quad (\text{A.1})$$

with a similar expression for the FT of $E_i(t)$. We can define a function $a(\omega)$ by the equation

$$\tilde{E}_i(\omega) = a(\omega) \tilde{E}_o(\omega). \quad (\text{A.2})$$

The function $a(\omega)$ is complex and is called the (electric) shielding factor or transfer function. The function can be obtained in principle from a knowledge of the two fields $E_o(t)$ and $E_i(t)$.

From physical arguments, it can be shown that $a(\omega)$ is an analytic function. Thus, if one has a set of analytic functions and a number of measured values of $a(\omega)$, it should be possible to obtain a fit that will provide a good approximation to the measured values and analytically continue the transfer function to complex values of ω outside the measurement region. The ability to effect this latter action is important because the range of ω covered in the experimental data is generally insufficient to determine the inverse transform integral that provides the internal electric field $E_i'(t)$ associated with an external field $E_o'(t)$ different from the experimental external field $E_o(t)$, where we would have

$$E_i'(t) = \frac{1}{2\pi} \int_{-\infty}^{\infty} \tilde{E}_o'(\omega) a(\omega) e^{-i\omega t} d\omega. \quad (\text{A.3})$$

We chose to accomplish this analytic fitting of the measured values of the transfer function by setting it equal to a linear superposition of analytic functions $f(\omega)$, where an individual such function is given by

$$f(\omega) = \frac{|A|e^{i\omega t_0}}{2} \left[\frac{e^{i\phi}}{(-i\omega - \alpha)^{n+1}} + \frac{e^{-i\phi}}{(-i\omega - \alpha^*)^{n+1}} \right], \quad (\text{A.4})$$

where the parameters t_0 , n , $|A|$, ϕ , and (complex) α are all selectable for each $f(\omega)$. To simplify the fitting chore for this study, we elected to restrict the values of some of these parameters by setting n equal to 1 and t_0 equal to zero and restricting ϕ to either 0 or π . The resulting set of functions was found to be sufficiently complete for our purposes so that only a small number of terms provided quite good fits to the data. One reason for this restriction is that the integral in Equation (A.3) can then be expressed in a simple closed form when $E_o'(t)$ is either the single-exponential or double-exponential external driving field of interest to us.

As mentioned above, the transfer function $a(\omega)$ is a complex quantity. But the data available in this and many other studies give information on only the absolute value of the function. For example, the data points of Figure 3-1 of this report represent values for the quantity

$$-20 \log | a(\omega) |.$$

Thus, our fitting job is somewhat more difficult than merely finding the best linear fit to the real and imaginary parts of $a(\omega)$; but, compared to some approaches, it was a very straightforward task.

As an exercise, we decided to see what differences would be introduced into the solutions presented in Section 3 of this report if we ignored the fact that the transfer function is a complex analytic function. In this exercise, we merely replaced the transfer function $a(\omega)$ with its absolute value in Equation (A.3). We found the resulting electric fields within Building Type 3 to be very close to those calculated by using the complex form for the transfer function, as far as peak field strength is concerned, but we noted differences in the late-time fields. These differences seemed to have only a modest effect on the predicted peak cable currents inside the building in most cases. However, for the case of a 10-meter cable strung two meters above the imperfectly reflecting floor treated in Section 3, the neglect of the phase of the transfer function changed the expected peak current in this cable by a factor of two.

In another exercise, we attempted to determine what would happen if we not only ignored the complex nature of the transfer function but also merely read the absolute values of the transfer function off the graph, rather than calculating them from an analytic fit. In this case, we used a discrete Fourier transform and inverse to calculate the time-domain electric field seen within Building Type 3 when a single-exponential field is incident upon the structure. The resulting peak internal electric field was calculated to be more than three times as large as that obtained from use of an analytic, complex transfer function. Thus, we conclude that, although there are many cases where the simplified approach of using a real transfer function will yield results quite similar to those obtained from the more detailed approach described here, it is recommended that any such use of the simpler model be subjected to a "sanity check" with the more detailed approach.

APPENDIX B

CABLE CURRENT CALCULATIONS

In this study, we used a transmission-line approach to calculate currents on cables exposed to incident EM fields. Specifically, the excitation of a cable was treated as a transmission line operating in the differential mode where the cable represents one line and the ground (conducting current in the opposite direction) represents the other line. The equations of such a system are given below.

Consider a transmission line strung in the z direction. For this case the transmission-line equations take the form

$$\frac{dV}{dz} = E_z - IZ$$

$$\frac{dI}{dz} = -VY,$$

where

V is the voltage between the lines,

I is the current on one line,

E_z is the external field parallel to the transmission line,

Z is the impedance per unit length, and

Y is the admittance per unit length.

For a cable beginning at $z = z_1$ and ending at $z = z_2$, the solution is given by

$$I(z) = [K_1 + P(z)]e^{-\gamma z} + [K_2 + Q(z)]e^{\gamma z}$$

$$V(z) = Z_0 \left\{ [K_1 + P(z)]e^{-\gamma z} - [K_2 + Q(z)]e^{\gamma z} \right\},$$

where

Z_0 is the characteristic impedance $(377/2\pi) \ln 2h/a$ (ohms);

γ is the propagation constant given by

$$j \frac{\epsilon}{c} \left[1 + \frac{1}{2 \ln \frac{2h}{a}} \left\{ \ln \left(\frac{1 + \sqrt{j \omega \tau_h}}{\sqrt{j \omega \tau_h}} \right) \right\} \right] \text{ (m}^{-1}\text{);}$$

$$P(z) = \frac{1}{2Z_0} \int_{z_1}^z E_z e^{\gamma z'} dz';$$

$$Q(z) = \frac{1}{2Z_0} \int_z^{z_2} E_z e^{-\gamma z'} dz';$$

$$K_1 = \rho_1 e^{\gamma z_1} \frac{\rho_2 P(z_2) e^{-\gamma z_2} - Q(z_1) e^{\gamma z_1}}{e^{\gamma(z_2-z_1)} - \rho_1 \rho_2 e^{-\gamma(z_2-z_1)}};$$

$$K_2 = \rho_2 e^{\gamma z_2} \frac{\rho_1 Q(z_1) e^{-\gamma z_1} - P(z_2) e^{\gamma z_2}}{e^{\gamma(z_2-z_1)} - \rho_1 \rho_2 e^{-\gamma(z_2-z_1)}};$$

$$\tau_h = \mu \sigma^2 h \quad (\text{seconds});$$

$$\rho_1 = (Z_1 - Z_0)/(Z_1 + Z_0);$$

$$\rho_2 = (Z_2 - Z_0)/(Z_2 + Z_0);$$

h is the height of the cable (meters);

a is the radius of the cable (meters);

Z₁ is the terminating impedance at z₁ (ohms);

Z₂ is the terminating impedance at z₂ (ohms);

σ is the soil conductivity (mhos/meter); and

μ is the soil permeability, 4π × 10⁻⁷ H/meter.

In predicting cable currents in this report, we have taken z₁ = 0, z₂ = length of cable, Z₁ = 0 (for short-circuit currents), and Z₂ infinite (to represent the open end of the line). Cable impedance was ignored.

For most of our calculations, we set h=2 meters (representing a typical height of a cable above the floor of the trailer or ground plane), a=0.008 meter (representing a typical intra-office cable bundle), and σ = 0.01 mho-meter. As noted in the main text of the report, however, other cases were run representing a perfectly reflecting ground plane (equivalent to setting σ to an arbitrarily large value) and a non-reflecting (or absent) ground or floor.

END

4-87

DTIC